Spanish LHC Network Meeting
Universidad Autonoma de Madrid
May 9th, 2017

Photon (+jet) and diphoton production at the LHC with the ATLAS detector

J. Terrón (Universidad Autónoma de Madrid)

On behalf of the ATLAS UAM team

- **Outline**
  - → Physics with photons
  - → Inclusive photon production at 8 TeV
  - → Photon + jet(s) production at 8 TeV
  - → Photon pair production at 8 TeV
  - → Inclusive photon production at 13 TeV
  - → Summary

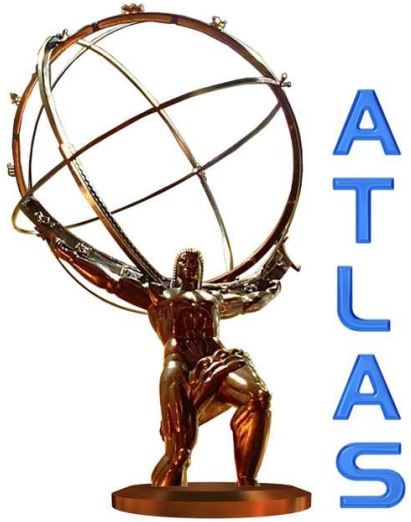

Photon production in pp collisions at LHC

- **Photon production in pp collisions allows**

$\rightarrow$ tests of perturbative QCD

$\rightarrow$ to extract information on the proton PDFs

- **Possibilities to study inclusive production of photons or in association with jets**

- **Prompt photons represent a cleaner probe of the hard interaction than jet production**

- **Aid searches involving photons or $E_{\mathrm{T}}^{\mathrm{miss}}$+jets (through ratios Z+jets/γ+jets)**

- **Diphoton production is of special interest as the major background to $H \rightarrow \gamma\gamma$**

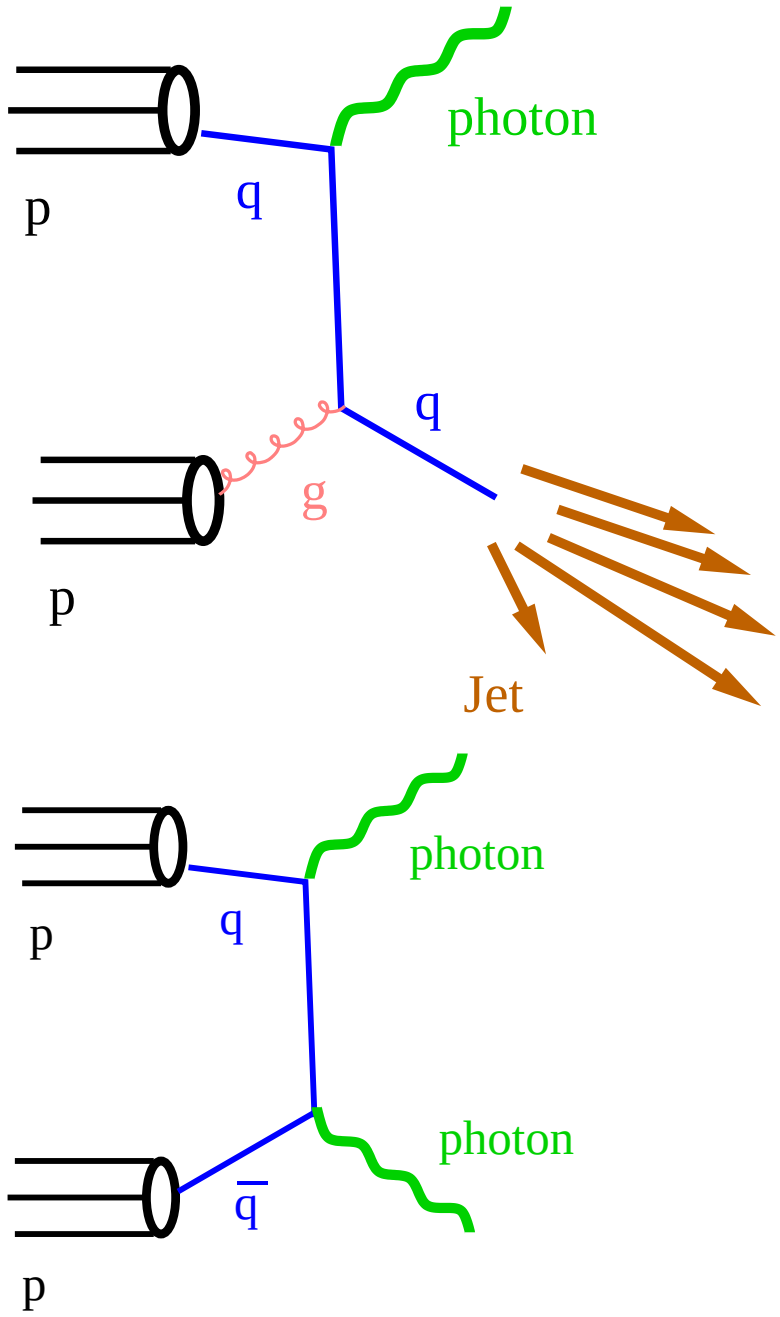

Inclusive photon production at 8 TeV

Inclusive isolated-photon production in pp collisions at $\sqrt{s} = 8$ TeV

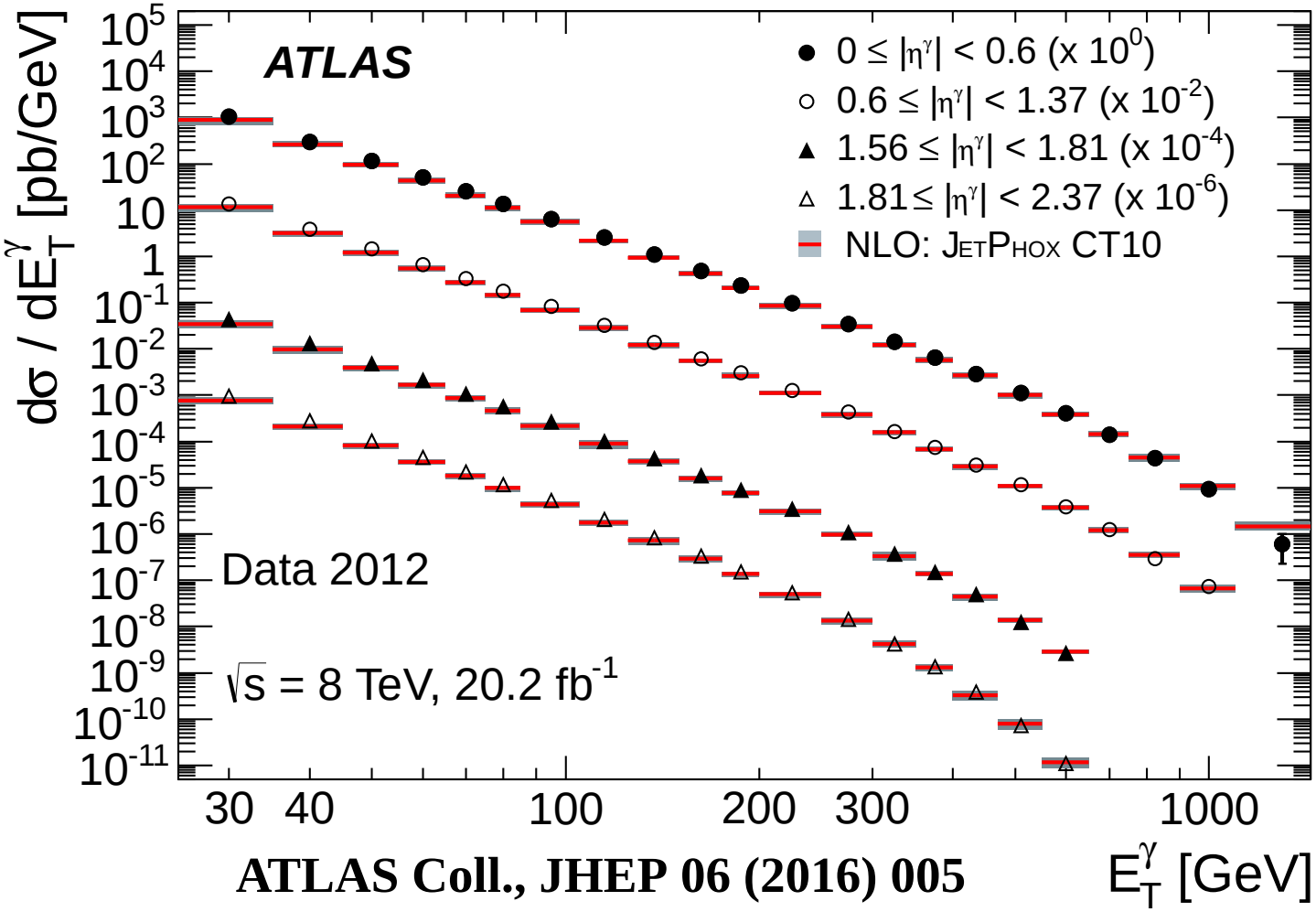

- Measurement of $d\sigma/dE_T^\gamma$ for $25 < E_T^\gamma < 1500$ GeV and different ranges in η^γ using $\mathcal{L} = 20.2$ fb^{-1} of pp collision data at $\sqrt{s} = 8$ TeV

$E_T^{\text{iso}} < 4.2 \cdot 10^{-3} \cdot E_T^\gamma + 4.8$ GeV

- The measurement covers ten orders of magnitude in cross section
- First measurement of photon production with $E_T^\gamma > 1$ TeV

- Significant improvement in experimental uncertainties over the previous measurements
- Good description (in log scale) of the data by NLO QCD calculations using JetPhox

Major experimental uncertainties

ATLAS Coll., JHEP 06 (2016) 005

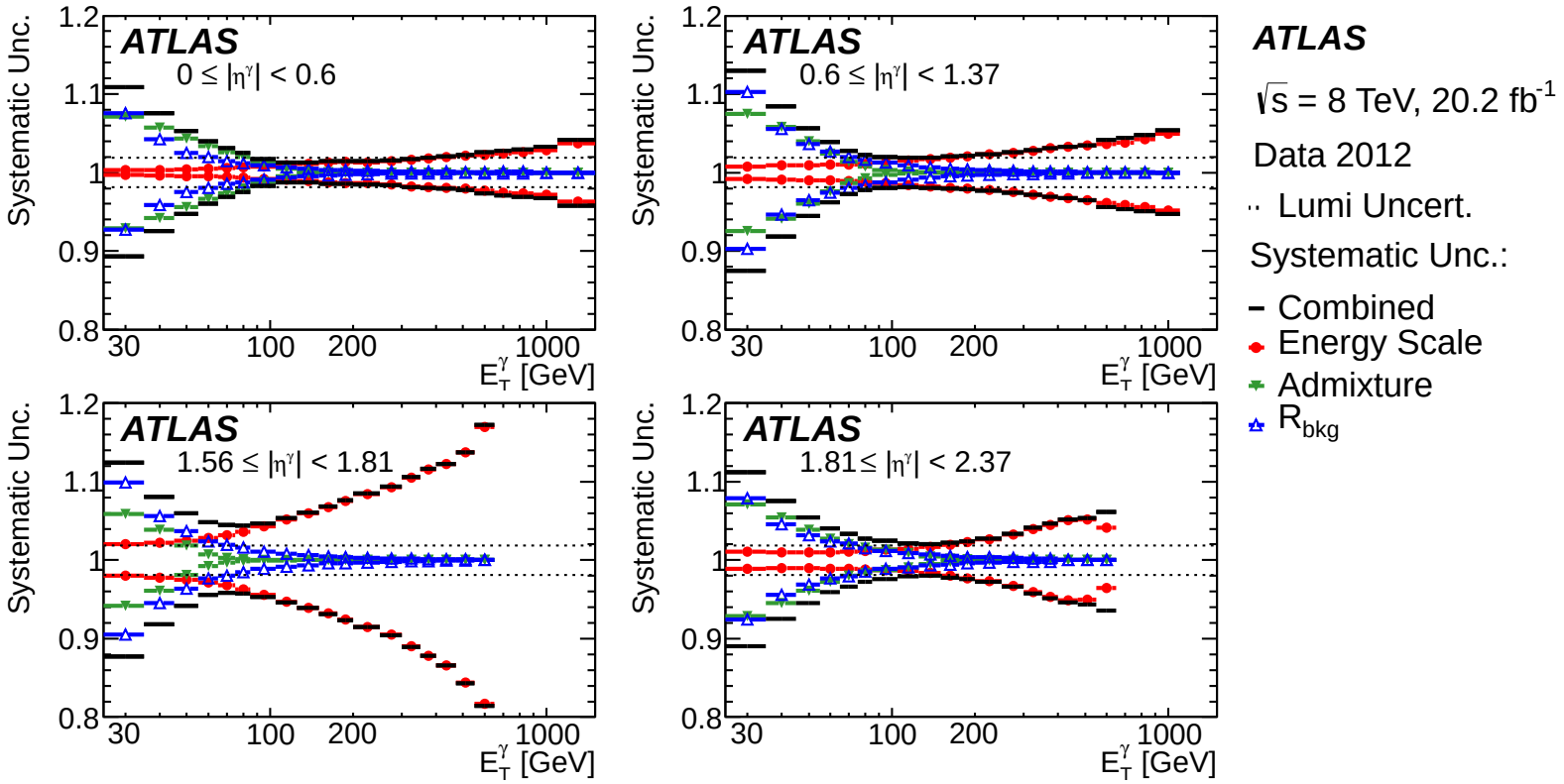

- **The uncertainty on the photon energy scale* (about 1% except in the region $1.56 < |\eta^\gamma| < 1.81$) is dominant at high E_T^γ**

* (ATLAS Collaboration, Eur. Phys. J. C74 (2014) 3071)

- **The uncertainty on the correlation in the background ($\pm 10\%$) dominates at low E_T^γ, but negligible at high E_T^γ**
- **The uncertainty on the admixture of direct and fragmentation photons increases at low E_T^γ**

Inclusive isolated-photon cross sections vs NLO QCD

ATLAS Coll., JHEP 06 (2016) 005

Theoretical uncertainties much larger than(!) experimental uncertainties

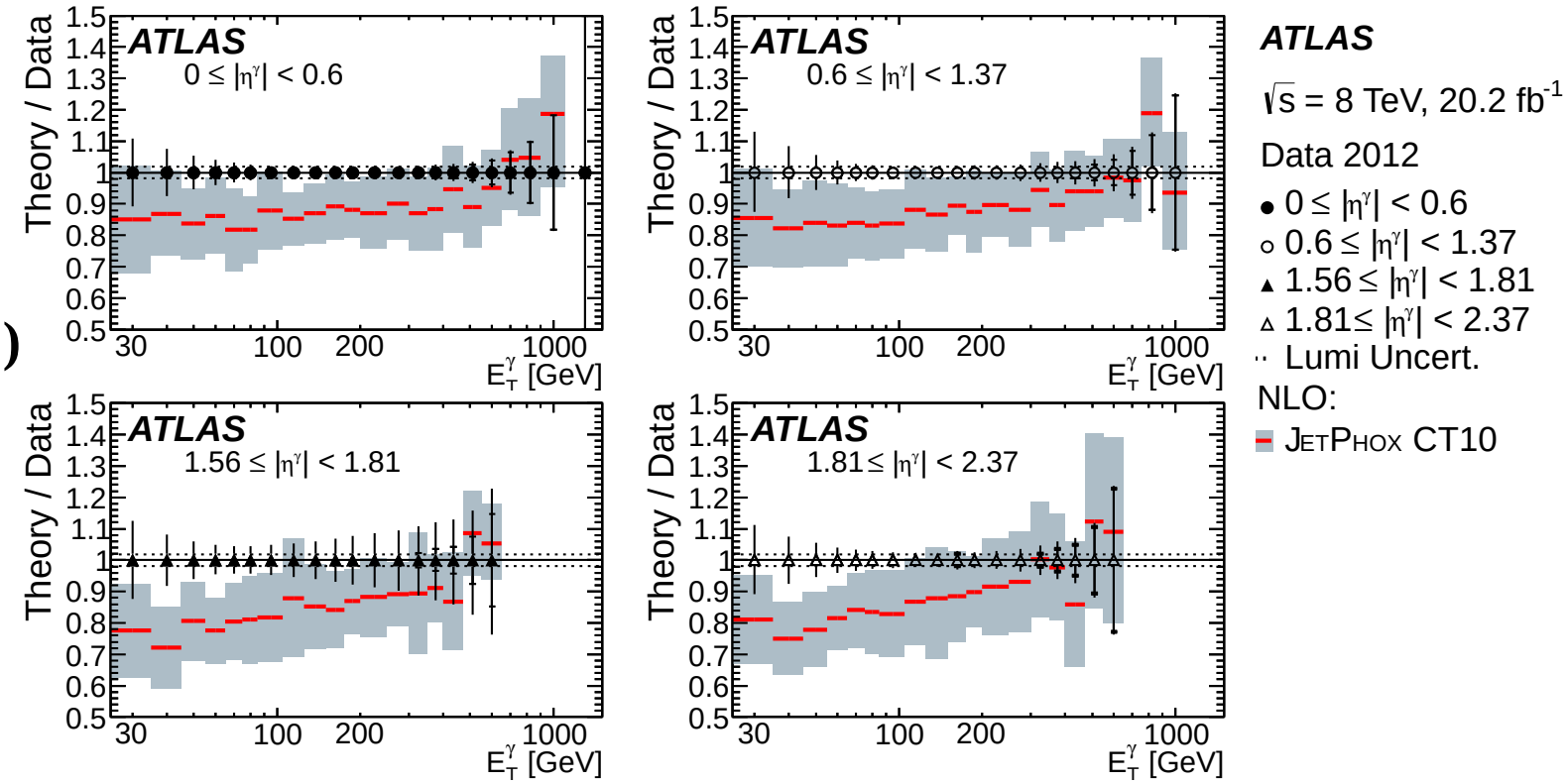

- **Comparison to NLO QCD calculation using the JetPhox program**
  - → a similar trend is observed at low E_T^γ in all $|\eta^\gamma|$ regions, the NLO QCD predictions underestimate the data by $\approx 20\%$
  - → the theoretical uncertainty (12-20%) prevents a more precise test of the SM predictions
- **Halving the measured uncertainties compared to previous measurements**
  - ⇒ useful constraint on proton PDFs once included in a global fit

Photon+jet(s) production at 8 TeV

Dynamics of $\gamma + \text{jet}$ production in pp collisions at $\sqrt{s} = 8$ TeV

- Study of the $\gamma + \text{jet}$ dynamics by measuring the differential cross sections as functions of
  - $\rightarrow$ Photon: E_T^γ
  - $\rightarrow$ Leading jet: p_T^{jet1}
  - $\rightarrow$ Photon+Leading jet: $m^{\gamma-jet1}$, $\cos\theta^*$

  where $\cos\theta^* = \tanh\frac{1}{2}(y^{\text{jet1}} - \eta^\gamma)$

  θ^* = scattering angle in centre-of-mass frame for $2 \rightarrow 2$ hard collinear scattering

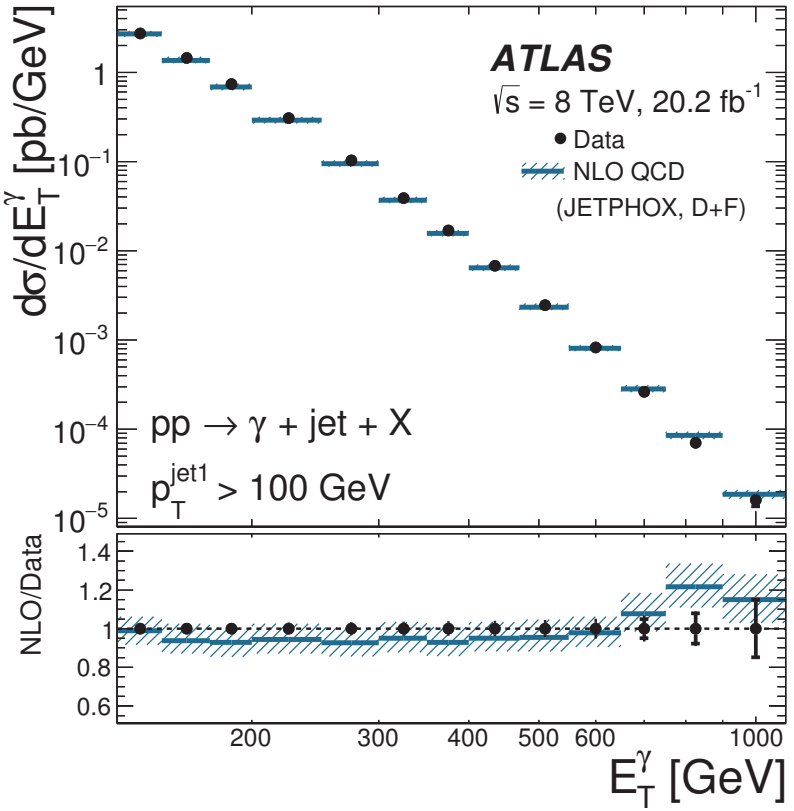

ATLAS Coll., NPB918 (2017) 257

- Measurements in the phase-space region defined by: $E_T^\gamma > 130$ GeV, $|\eta^\gamma| < 2.37$ (excluding the region $1.37 < |\eta^\gamma| < 1.56$), $p_T^{jet1} > 100$ GeV, $|y^{\text{jet1}}| < 4.4$ (anti-k_t algorithm with $R = 0.6$), $E_T^{\text{iso}} < 10$ GeV and $\Delta R_{\gamma j} > 1$
- Comparison to NLO QCD calculation (JETPHOX) corrected for non-perturbative effects
- Good description of the measured $d\sigma/dE_T^\gamma$ by the NLO QCD calculations

Dynamics of γ + jet production in pp collisions

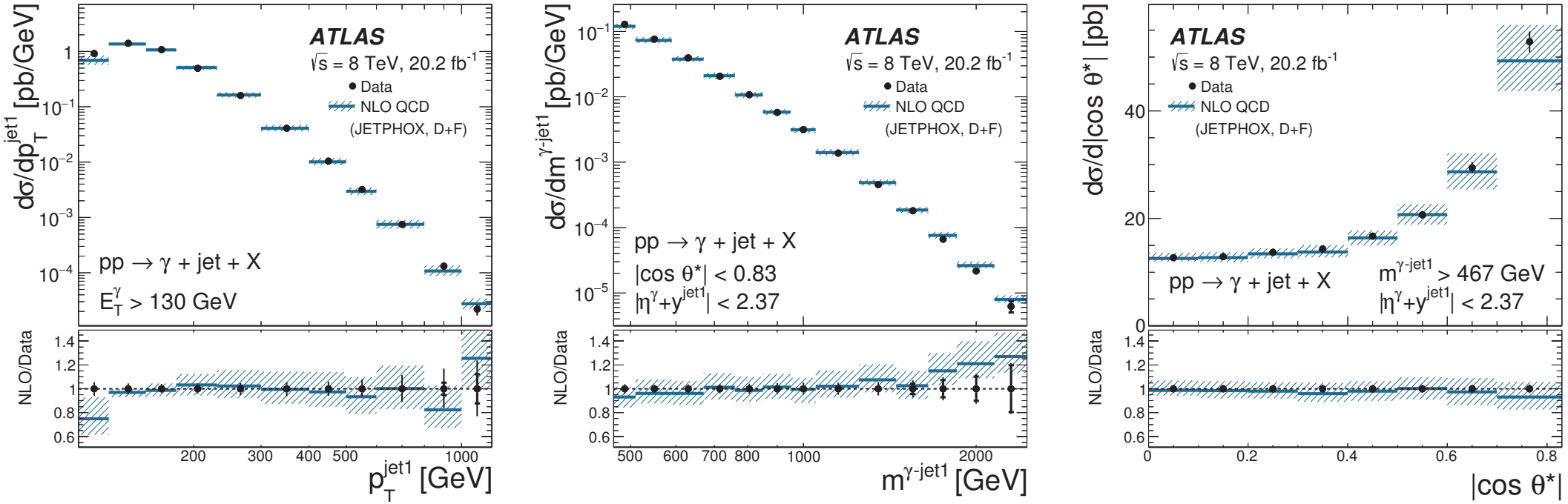

ATLAS Coll., NPB918 (2017) 257

- **Additional requirements for $d\sigma/dm^{\gamma-jet1}$ and $d\sigma/d|\cos\theta^*|$ to remove biases:**

$$|\eta^{\gamma} + y^{jet1}| < 2.37 \;\; , \;\; |\cos\theta^*| < 0.83 \;\; , \;\; m^{\gamma-jet1} > 467 \text{ GeV}$$

- **In the selected (unbiased) region the angular distribution increases as $|\cos\theta^*|$ increases**
- **Good description of the data by the NLO QCD calculations within the (small) experimental and theoretical uncertainties $\Rightarrow$ validation of the description of the dynamics of γ + jet production in pp collisions at $\mathcal{O}(\alpha_{em}\alpha_s^2)$**

Dynamics of γ + jet production in pp collisions

ATLAS Coll., NPB918 (2017) 257

- **Angular distribution $d\sigma/d|\cos\theta^{\gamma j}|$ sensitive to the spin of the exchanged (virtual) particle: quark(1/2) vs gluon(1)**

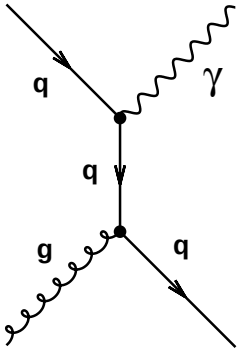

direct-photon process

$$d\sigma/d|\cos\theta^{\gamma j}| \sim \sim (1-|\cos\theta^{\gamma j}|)^{-1}$$

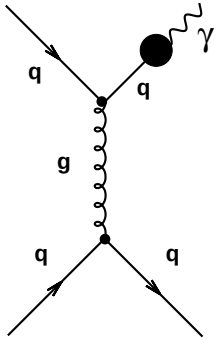

fragmentation process

$$d\sigma/d|\cos\theta^{\gamma j}| \sim \sim (1-|\cos\theta^{\gamma j}|)^{-2}$$

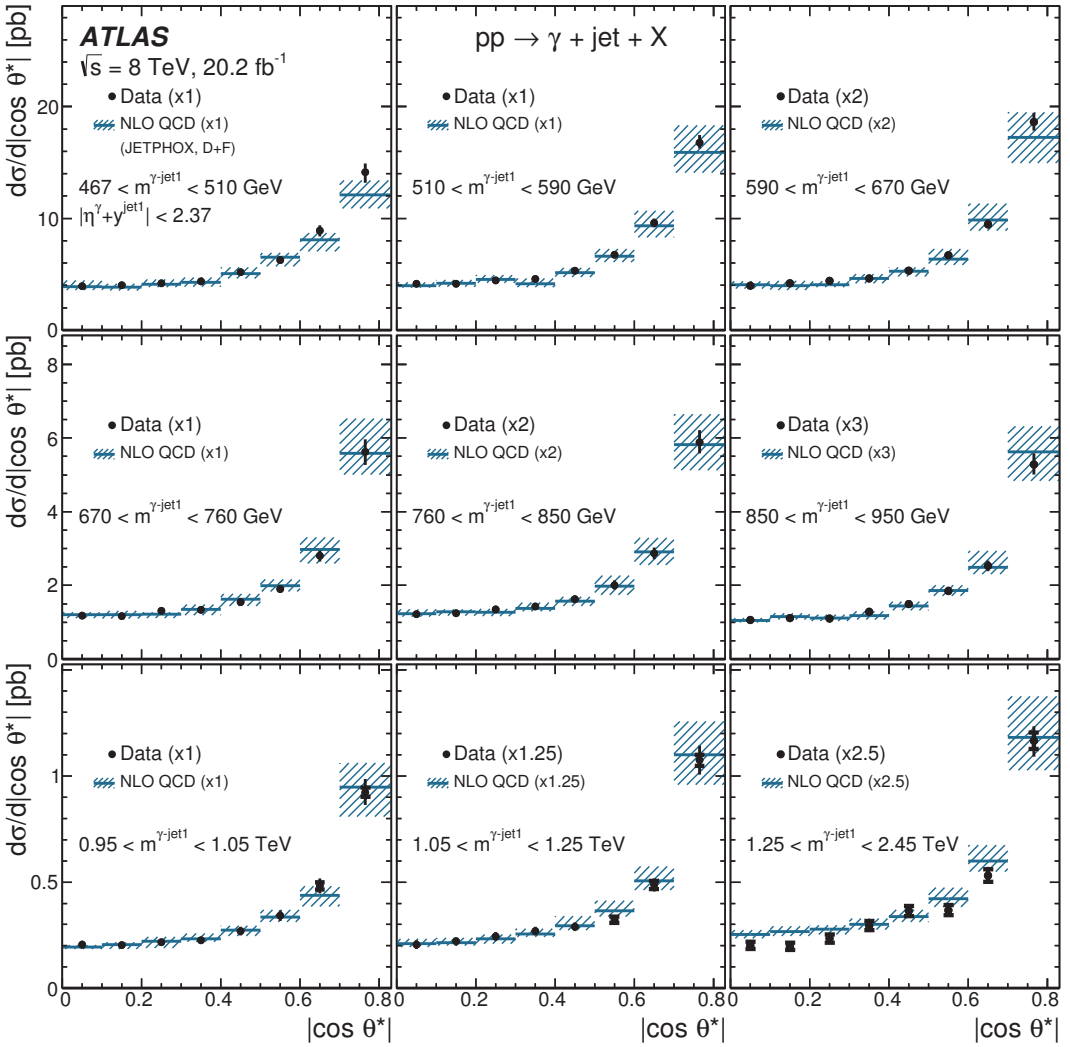

- **Measured angular distribution in regions of photon-jet invariant mass**

$\Rightarrow$ good description of the data by NLO QCD in shape and normalisation

Dynamics of γ + jet production in pp collisions

ATLAS Coll., NPB918 (2017) 257

- **Angular distribution $d\sigma/d|\cos\theta^{\gamma j}|$ sensitive to the spin of the exchanged (virtual) particle: quark(1/2) vs gluon(1)**

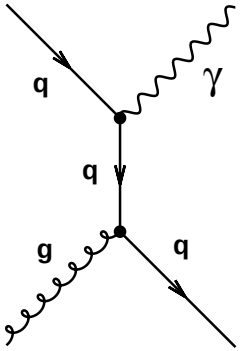

direct-photon process

$$d\sigma/d|\cos\theta^{\gamma j}| \sim$$
$$\sim (1-|\cos\theta^{\gamma j}|)^{-1}$$

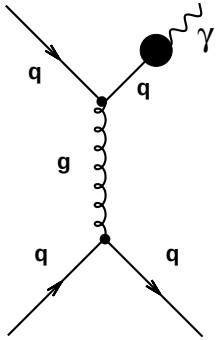

fragmentation process

$$d\sigma/d|\cos\theta^{\gamma j}| \sim$$
$$\sim (1-|\cos\theta^{\gamma j}|)^{-2}$$

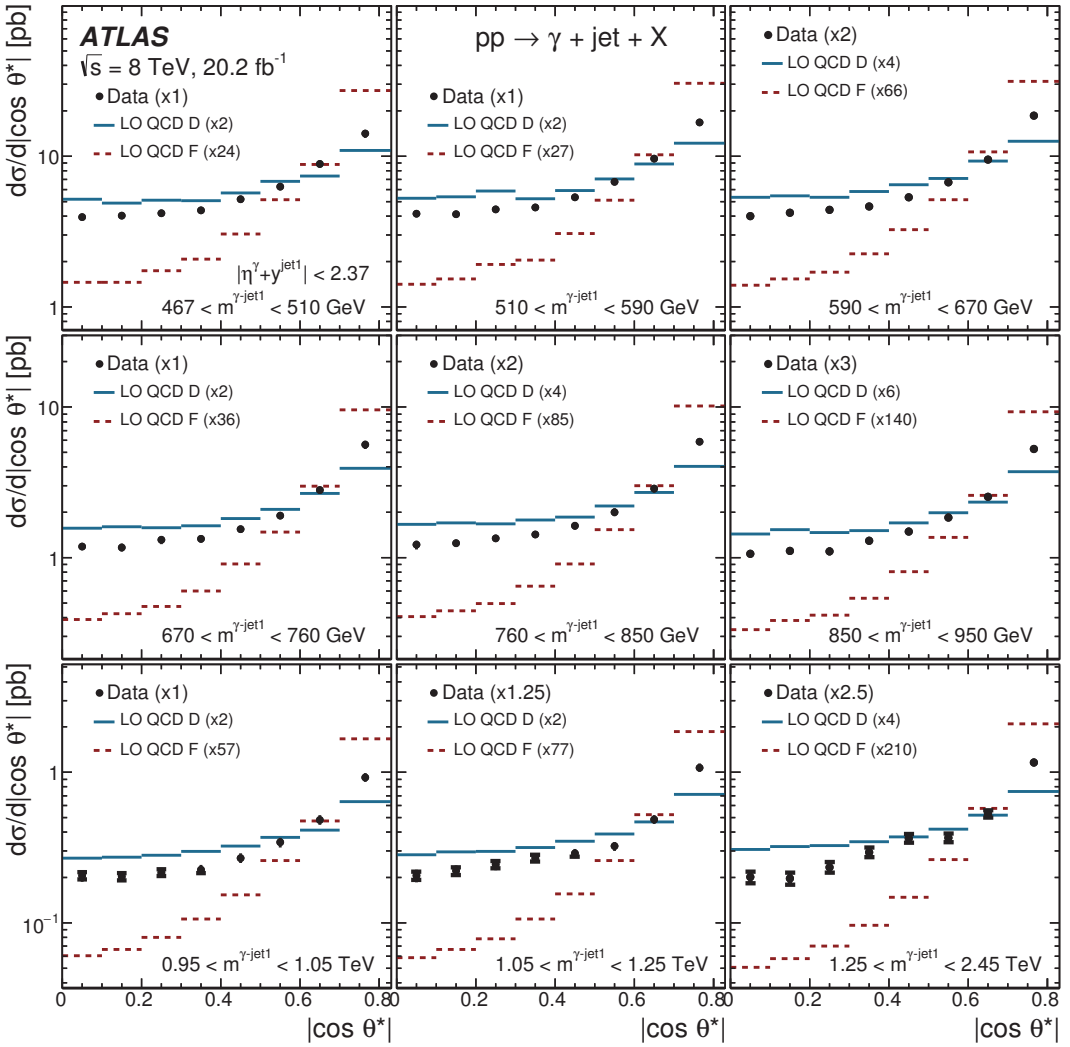

- **Measured angular distribution closer to that of direct-photon processes than fragm.**

$\Rightarrow$ consistent with the dominance of processes in which a virtual quark is exchanged

Dynamics of $\gamma + 2\text{jet}$ production in pp collisions

ATLAS Coll., NPB918 (2017) 257

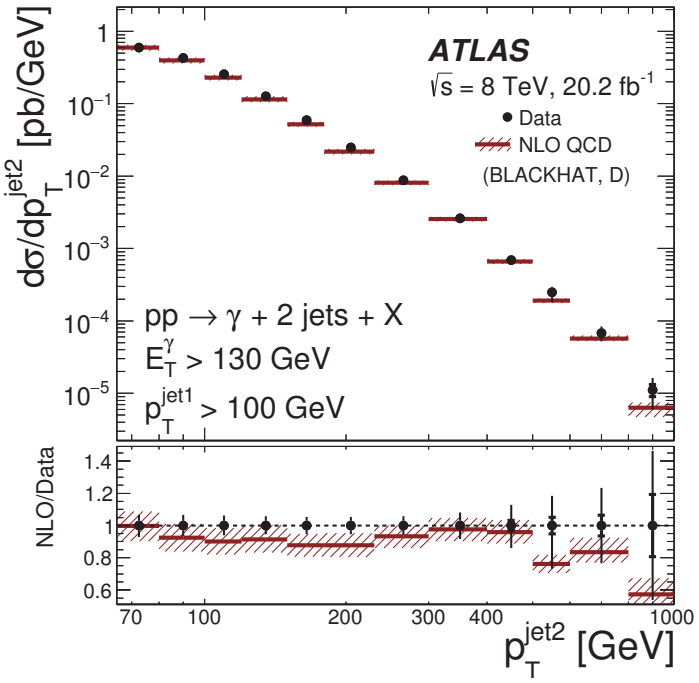

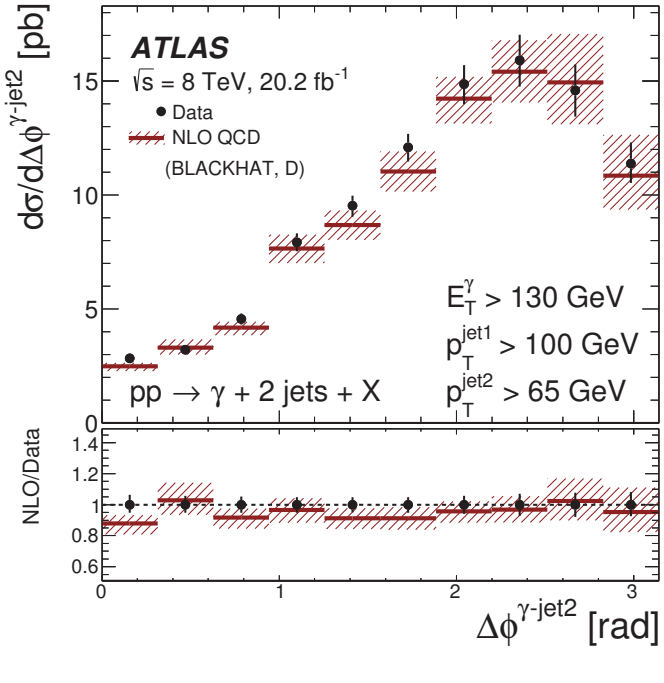

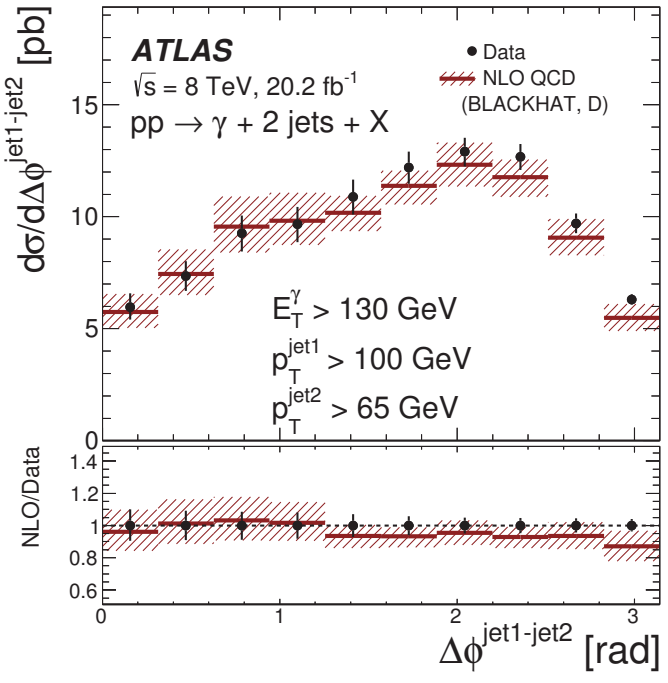

- **First measurement of $\gamma + 2\text{jet}$ production in pp collisions at $\sqrt{s} = 8$ TeV:**

  $E_T^{\gamma} > 130$ GeV, $p_T^{jet1} > 100$ GeV and $p_T^{jet2} > 65$ GeV

- **Measurement of $d\sigma/dp_T^{jet2}$ and angular correlations between the photon and the jets**

  $\rightarrow \Delta\phi$ between the photon and subleading jet ($\Delta\phi^{\gamma-jet2}$)

  $\rightarrow \Delta\phi$ between the leading and subleading jets ($\Delta\phi^{jet1-jet2}$)

- **Good description of the data both in shape and normalisation by the NLO QCD predictions computed with Blackhat**

Dynamics of $\gamma + 2\text{jet}$ production in pp collisions

ATLAS Coll., NPB918 (2017) 257

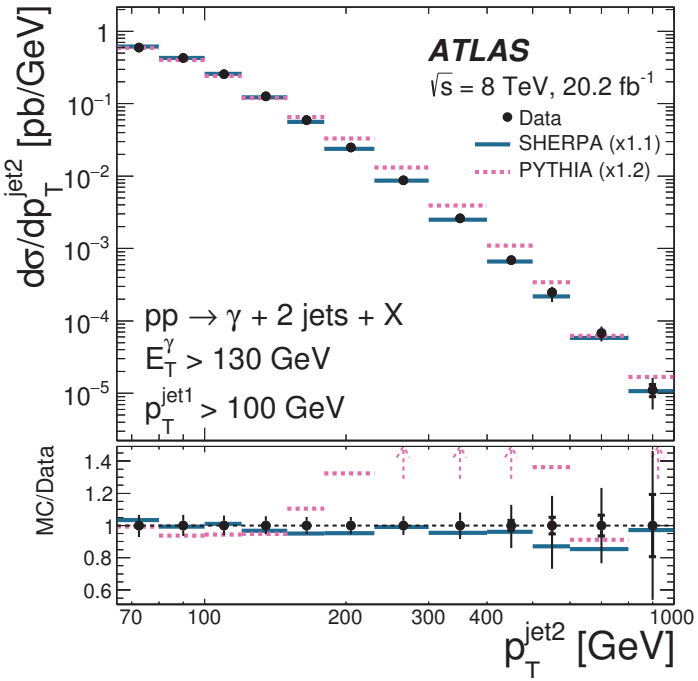

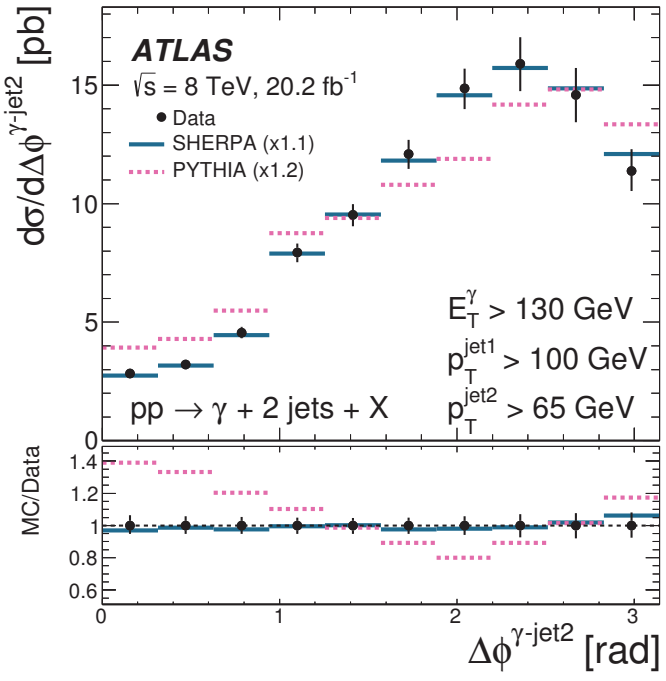

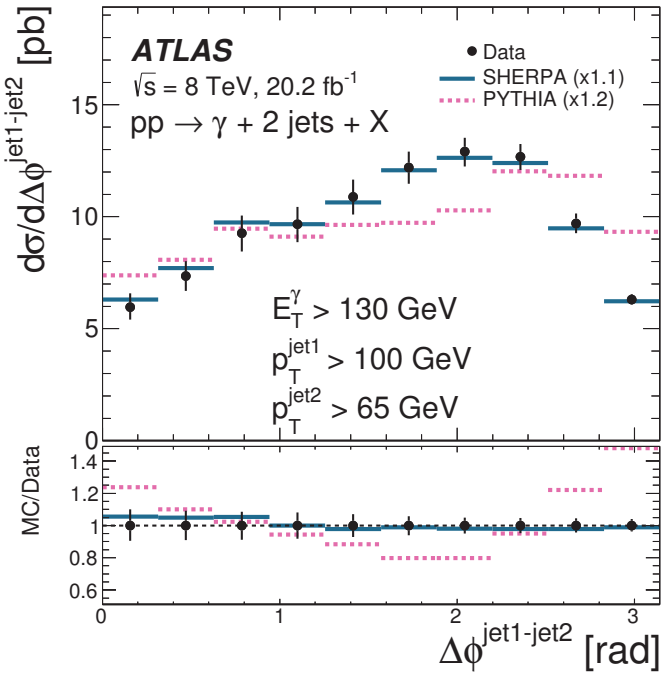

- **Comparison to the predictions of Monte Carlo generators:**
  - → **PYTHIA: $2 \to 2$ matrix elements plus parton showers**
  - → **SHERPA: $2 \to n$ ($n = 2, \ldots, 5$) matrix elements plus parton showers**
- **MC predictions normalised to data: shape comparison only**
- **Good description of the data by the SHERPA predictions while PYTHIA fails to describe the distribution in p_T^{jet2} and the angular correlations**

  ⇒ The inclusion of higher-order tree-level ME makes SHERPA superior!

Dynamics of $\gamma + 3\text{jet}$ production in pp collisions

ATLAS Coll., NPB918 (2017) 257

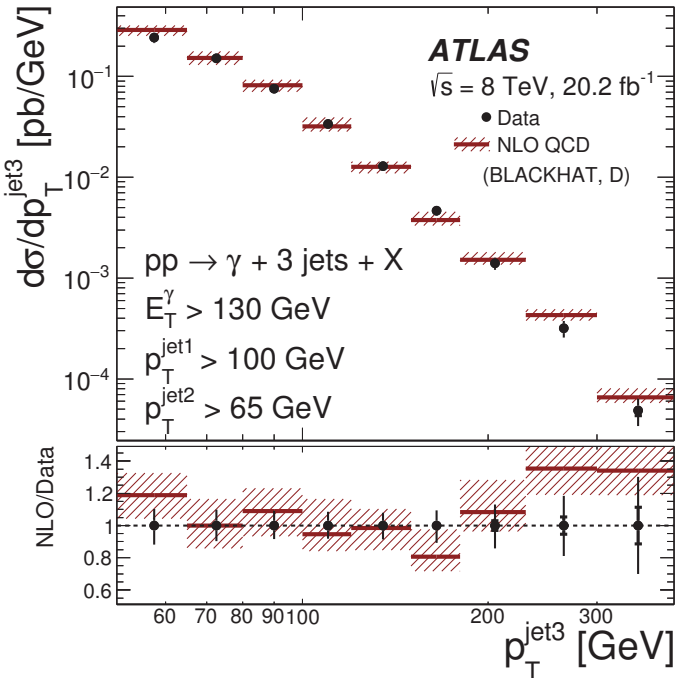

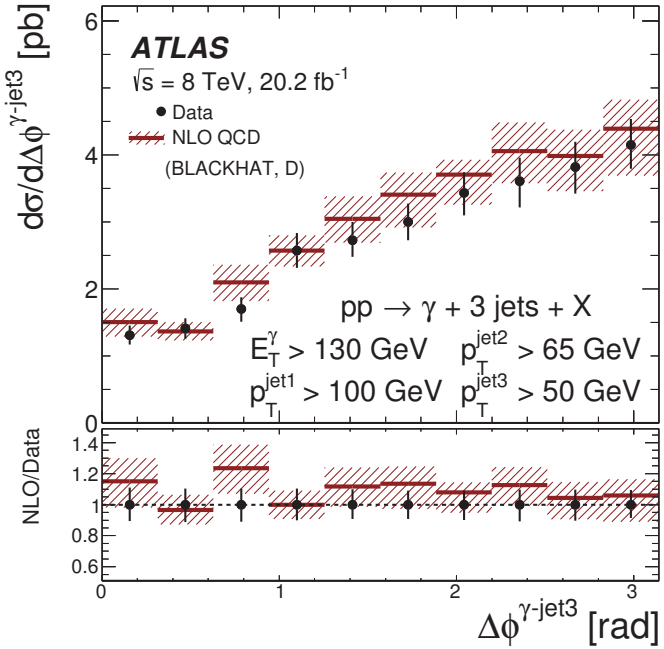

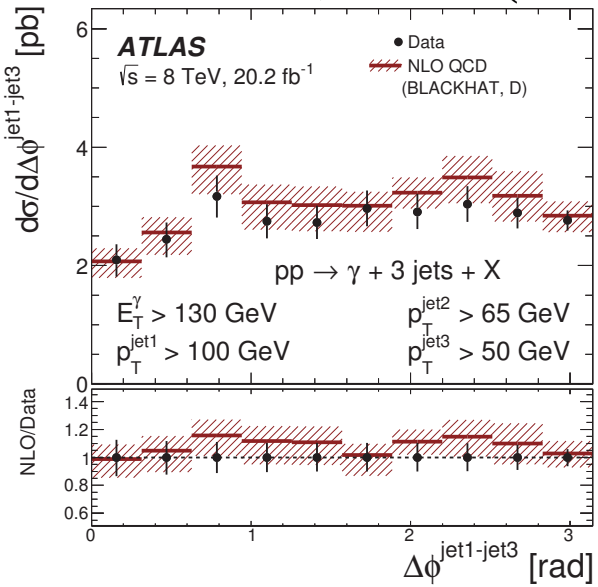

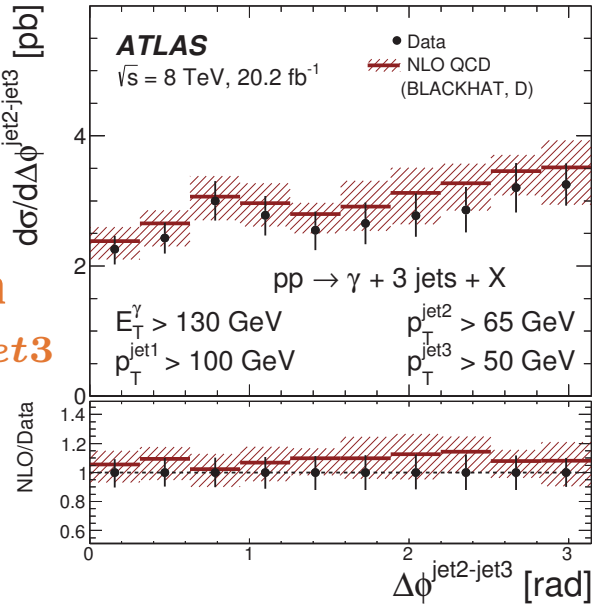

- **First measurement of $\gamma + 3\text{jet}$ at the LHC: $E_T^{\gamma} > 130$ GeV, $p_T^{jet1} > 100$ GeV, $p_T^{jet2} > 65$ GeV and $p_T^{jet3} > 50$ GeV**
- **Measurement of $d\sigma/dp_T^{jet3}$ and angular correlations between the photon and the jets: $\Delta\phi^{\gamma-jet3}$, $\Delta\phi^{jet1-jet3}$, $\Delta\phi^{jet2-jet3}$**
- **Adequate description of the data by the NLO QCD predictions computed with Blackhat**

Dynamics of $\gamma + 3\text{jet}$ production in pp collisions

ATLAS Coll., NPB918 (2017) 257

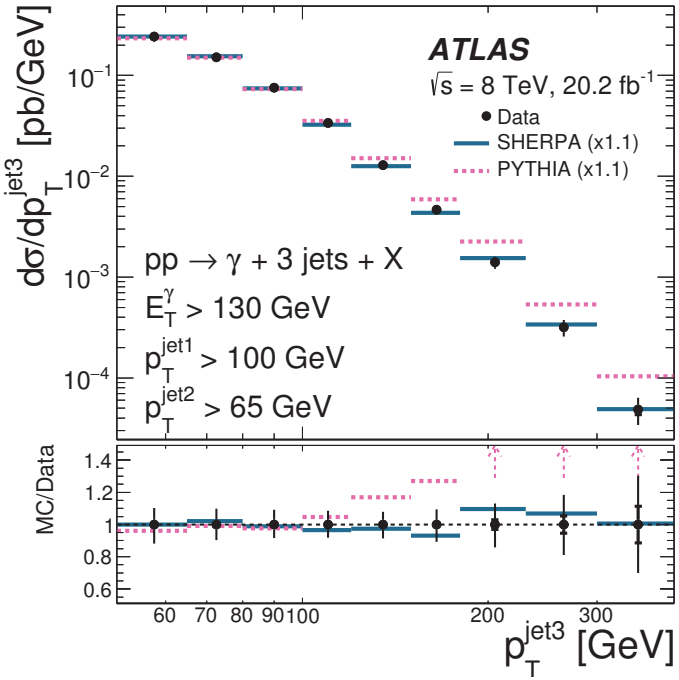

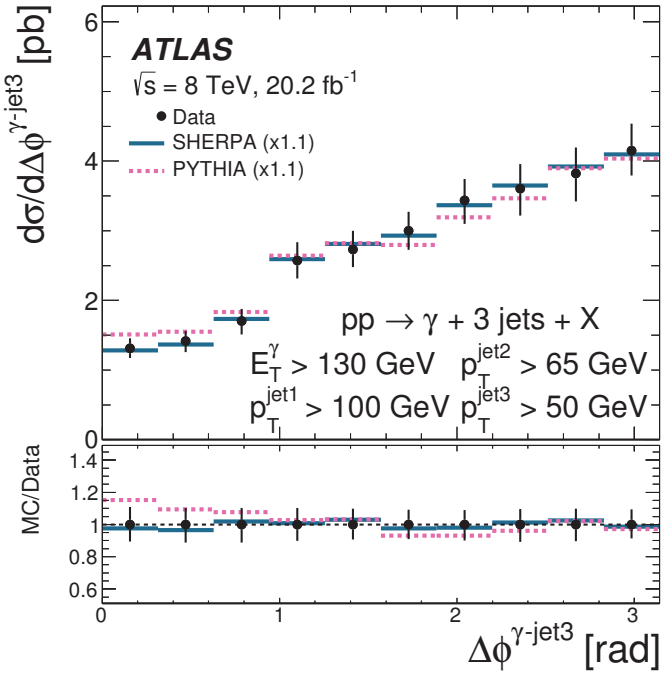

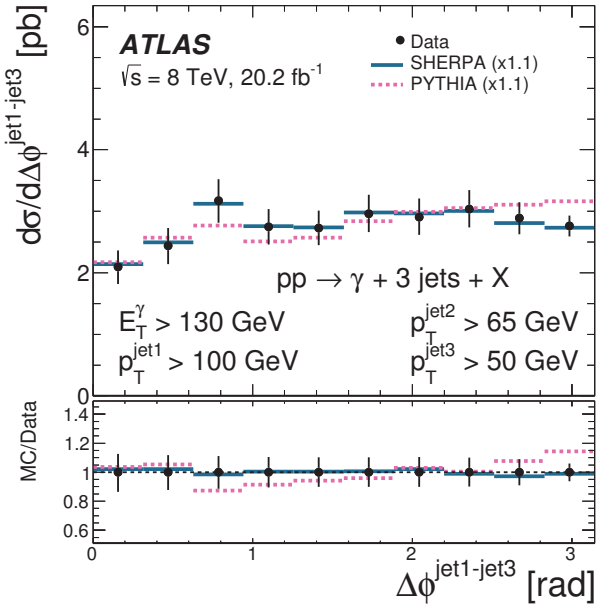

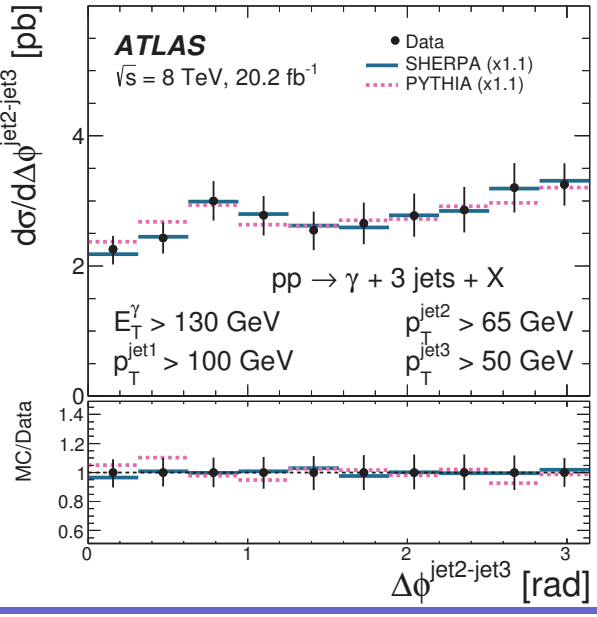

- **Comparison to the predictions of Monte Carlo generators of PYTHIA ($2 \to 2$ ME+PS) and SHERPA ($2 \to n$ ME +PS) normalised to data (shape comparison)**
- **Good description of the data by the SHERPA predictions while PYTHIA fails to describe the distribution in p_T^{jet3}**

$\Rightarrow$ The inclusion of higher-order tree-level ME makes SHERPA superior to PYTHIA

Photon pair production at 8 TeV

Isolated-photon pair production in pp collisions

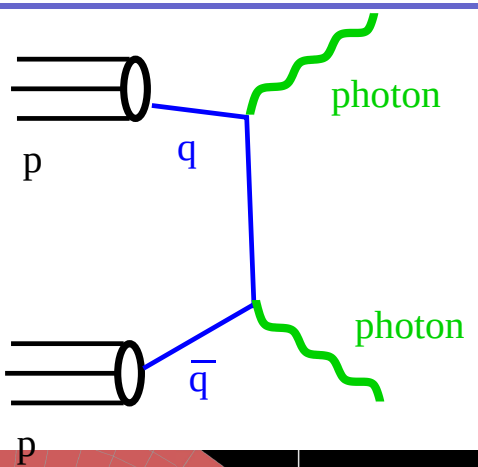

- Measurements of the process $pp \to \gamma\gamma + X$ with the aim of testing pQCD and understanding the irreducible background to new physics processes involving photons or $H \to \gamma\gamma$
- Measurement of differential cross sections

$\to$ diphoton invariant mass, $m_{\gamma\gamma}$

$\to$ diphoton transverse momentum, $p_{T,\gamma\gamma}$

$\to$ azimuthal separation in LAB frame, $\Delta\phi_{\gamma\gamma}$

$\to \cos\theta^*_\eta$ $\to \phi^*_\eta \equiv \tan\left(\frac{\pi - \Delta\phi_{\gamma\gamma}}{2}\right) \sin\theta^*_\eta$

$\to$ transverse component of $\vec{p}_{T,\gamma\gamma}$ with respect to thrust axis (a_T)

in the phase-space region defined by:

$E_T^{\gamma 1,2} > 40(30)$ GeV, $|\eta^\gamma| < 2.37$ (excluding the region $1.37 < |\eta^\gamma| < 1.56$), $\Delta R_{\gamma\gamma} > 0.4$ and $E_T^{iso} < 11$ GeV using $\mathcal{L} = 20.2\ \text{fb}^{-1}$

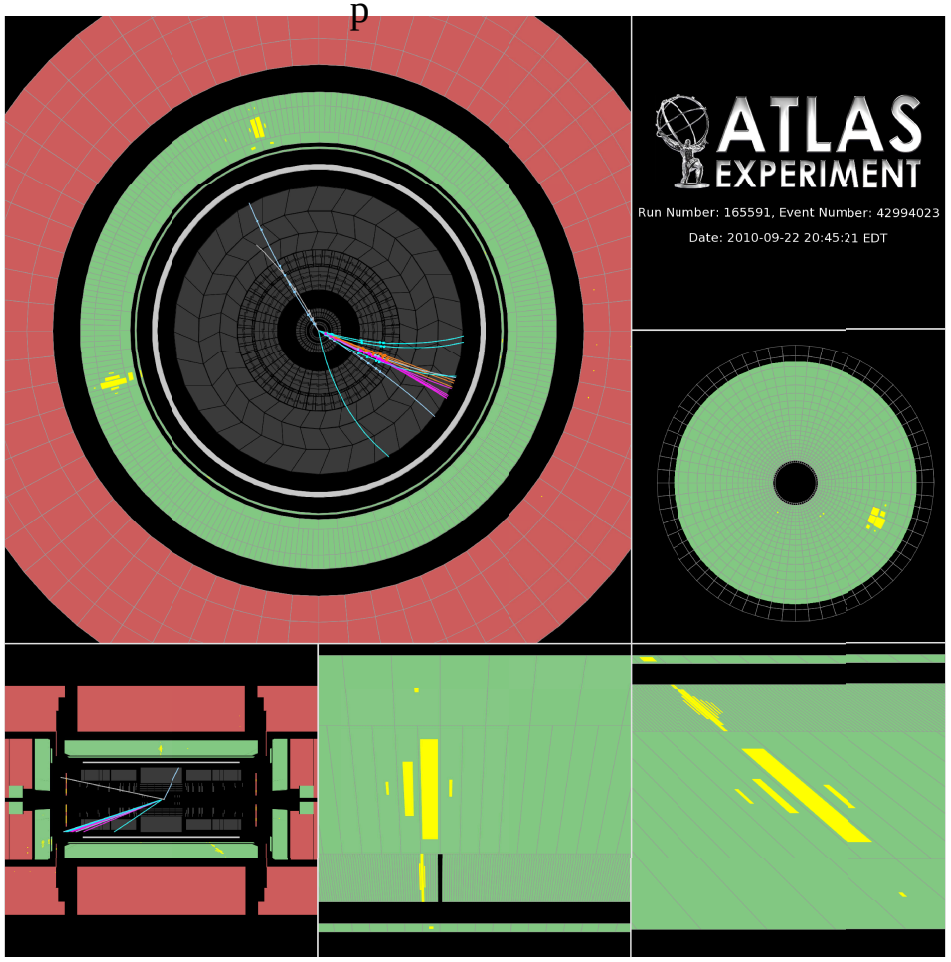

Isolated-photon pair production in pp collisions at $\sqrt{s} = 8$ TeV

- **Comparison to theoretical calculations**
- **Fixed-order QCD calculations (NP corrected)**
  - → 2γNNLO program; NNLO calculation of direct-photon contribution (no fragm.)
  - → DIPHOX program; NLO calculation of direct-photon and fragmentation contributions; box diagram $gg \to \gamma\gamma$ included
  - → RESBOS program; NLO plus NNLL resummation
- **New SHERPA (v2.2.1) calculation combining**
  - → $\gamma\gamma$ and $\gamma\gamma + 1\text{p}$ at NLO
  - → $\gamma\gamma + 2\text{p}$ and $\gamma\gamma + 3\text{p}$ at LO
  - → parton showers
- **The small contribution from $H \to \gamma\gamma$ is neglected**

⇒ **SHERPA prediction in agreement with data**

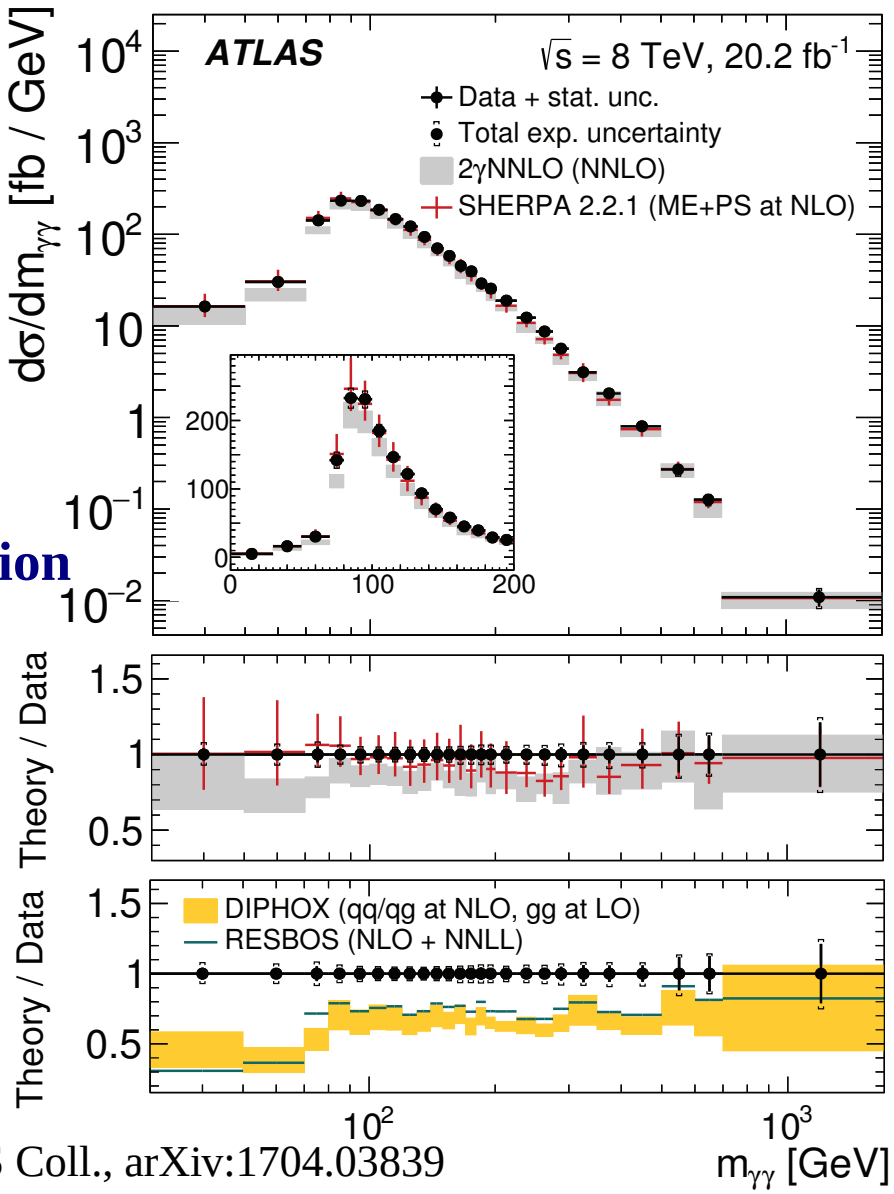

ATLAS Coll., arXiv:1704.03839

Isolated-photon pair production in pp collisions at $\sqrt{s} = 8$ TeV

- **Comparison to theoretical calculations**
- **Fixed-order QCD calculations (NP corrected)**
  - → 2γNNLO program; NNLO calculation of direct-photon contribution (no fragm.)
  - → DIPHOX program; NLO calculation of direct-photon and fragmentation contributions; box diagram $gg \to \gamma\gamma$ included
  - → RESBOS program; NLO plus NNLL resummation
- **New SHERPA (v2.2.1) calculation combining**
  - → $\gamma\gamma$ and $\gamma\gamma + 1\text{p}$ at NLO
  - → $\gamma\gamma + 2\text{p}$ and $\gamma\gamma + 3\text{p}$ at LO
  - → parton showers
- **The small contribution from $H \to \gamma\gamma$ is neglected**

⇒ **SHERPA prediction in agreement with data**

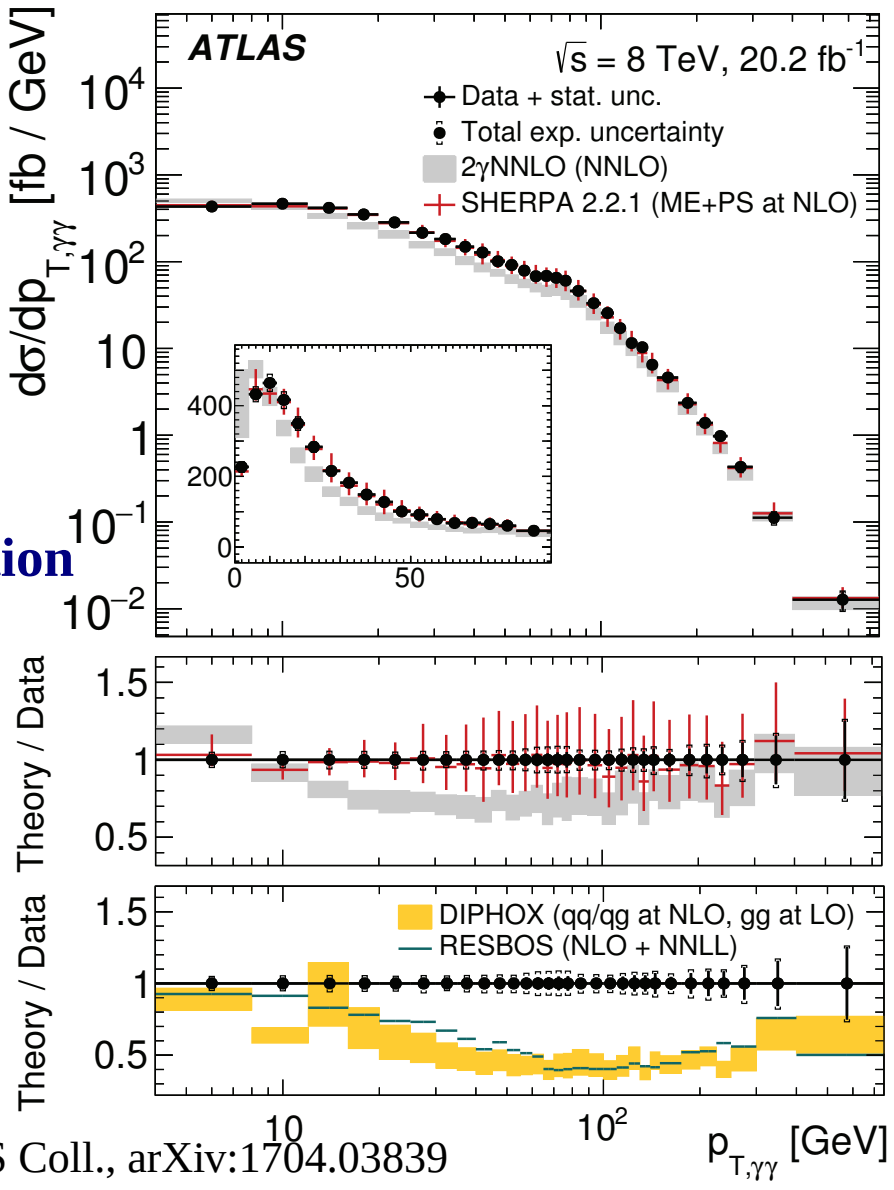

ATLAS Coll., arXiv:1704.03839

Isolated-photon pair production in pp collisions at $\sqrt{s} = 8$ TeV

ϕ^*_η a_T $|\cos\theta^*_\eta|$ $\Delta\phi_{\gamma\gamma}$

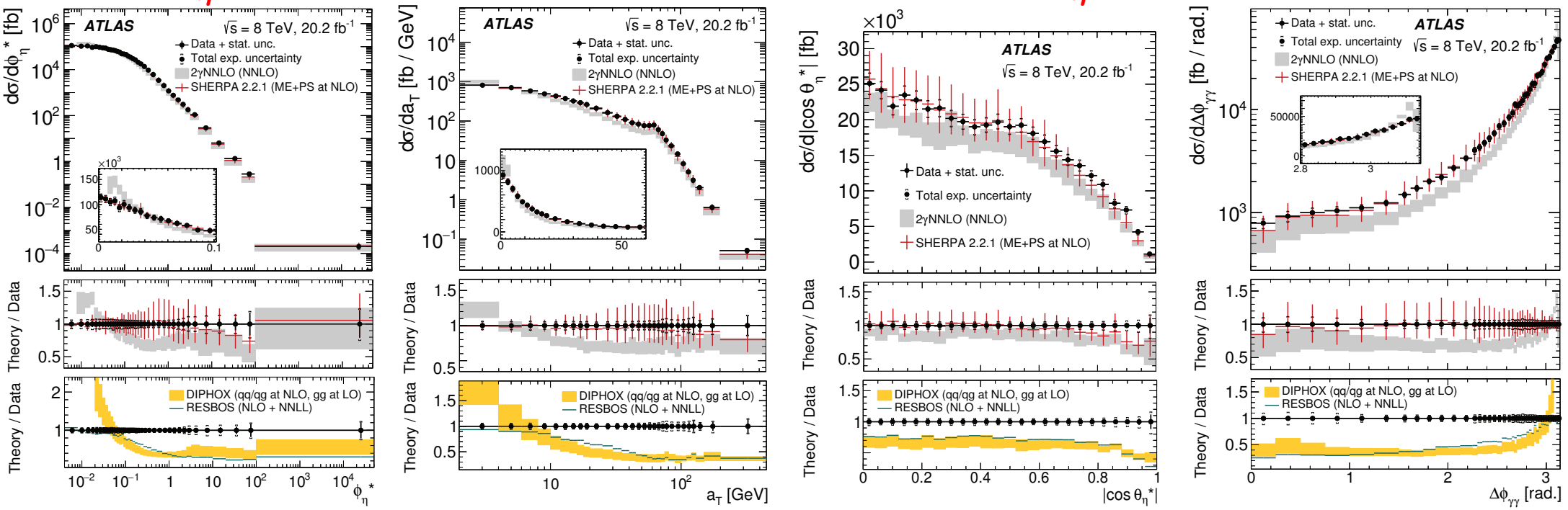

ATLAS Coll., arXiv:1704.03839

- $\Delta\phi_{\gamma\gamma} \sim \pi$ or at low values of $p_{T,\gamma\gamma}$, a_T and ϕ^*_η (soft gluon resummation important): **RESBOS** and **SHERPA** do well
- NLO QCD calculations without higher order terms (DIPHOX, RESBOS) are insufficient
- NNLO corrections (2γNNLO) improve the description, but still insufficient
- **SHERPA predictions agree with the data**

Inclusive photon production at 13 TeV

Inclusive isolated-photon production in pp collisions at $\sqrt{s} = 13$ TeV

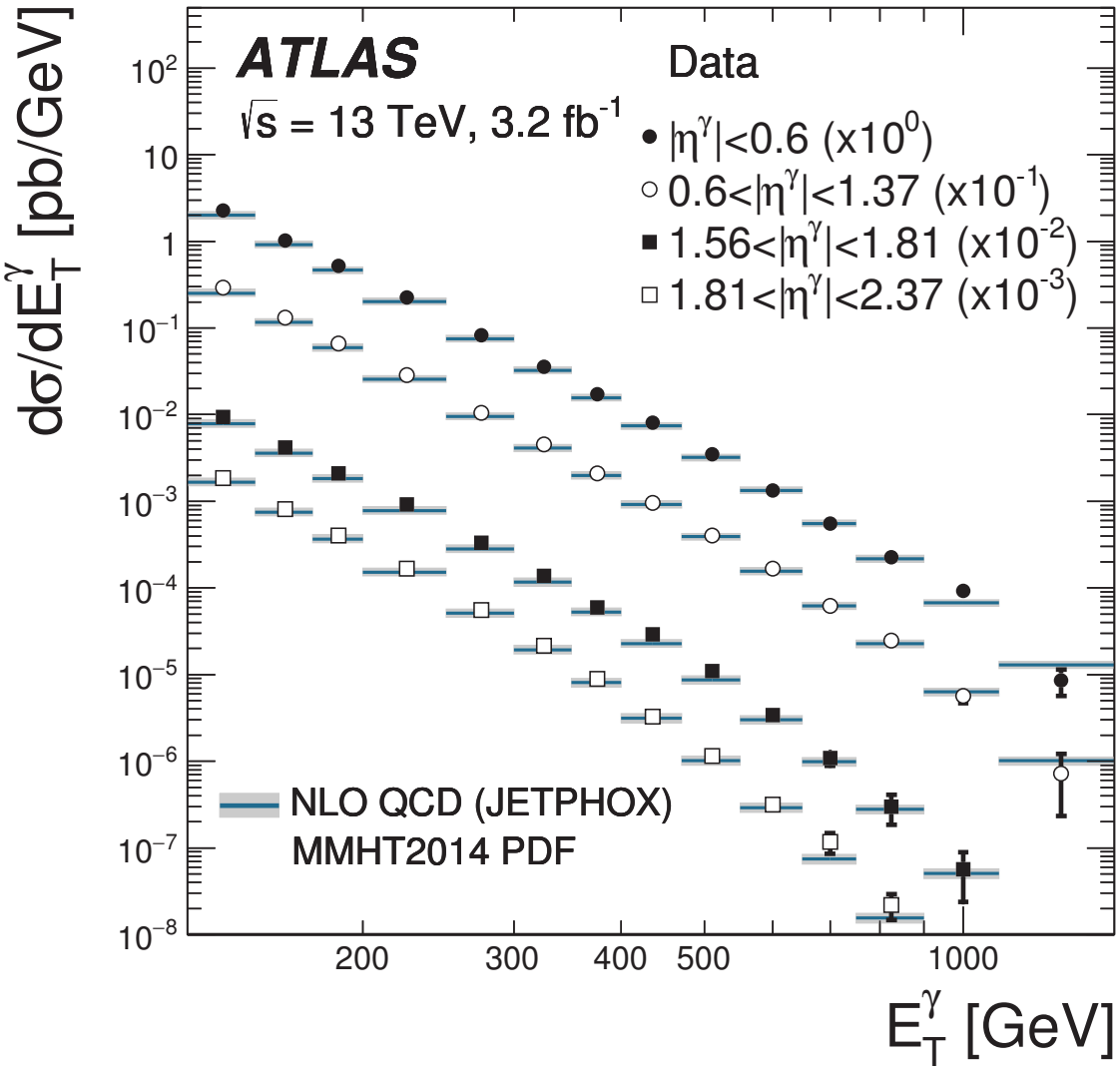

ATLAS Coll., arXiv:1701.06882, accepted PLB

- **Measurement of $d\sigma/dE_T^\gamma$ in different ranges in η^γ for $125 < E_T^\gamma < 1500$ GeV using $\mathcal{L} = 3.2$ fb^{-1} of pp collision data at $\sqrt{s} = 13$ TeV**
- **Isolation: $E_T^{\text{iso}} < 4.2 \cdot 10^{-3} \cdot E_T^\gamma + 4.8$ GeV**
- **The measurement covers more than five orders of magnitude in cross section**
- **$d\sigma/dE_T^\gamma$ increases by a factor 2 (10) at $E_T^\gamma = 125$ (1000) GeV with respect to at $\sqrt{s} = 8$ TeV**
- **Good description (in log scale) of the data by NLO QCD predictions computed with JetPhox using the MMHT2014 PDFs**

Major experimental uncertainties

ATLAS Coll., arXiv:1701.06882, accepted PLB

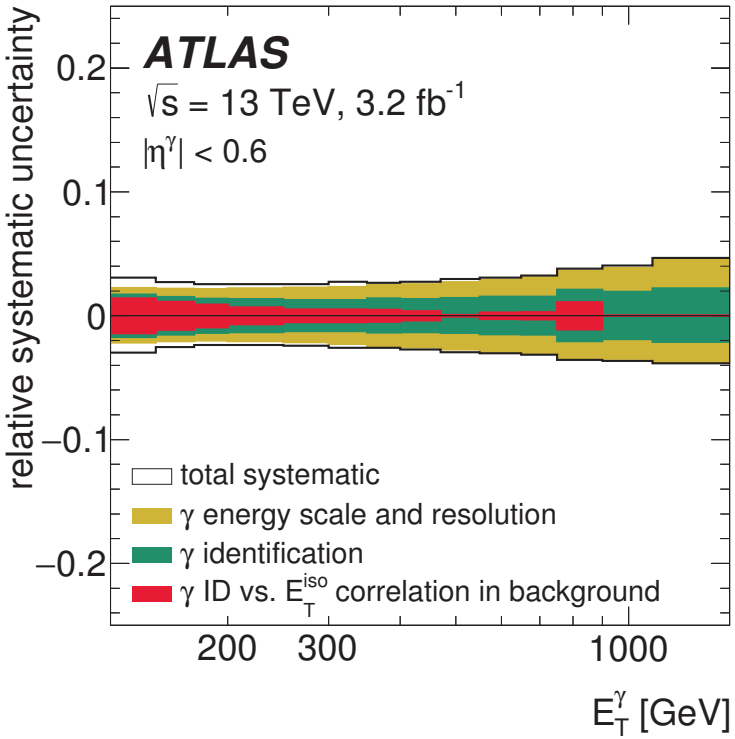

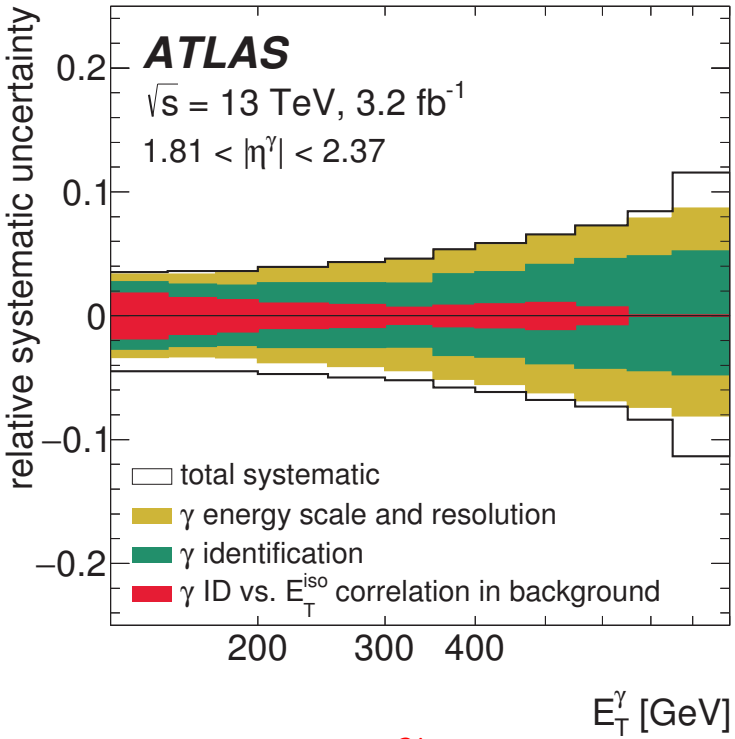

- **The uncertainty on the photon energy scale dominates at high E_T^γ: 2-5% except for $1.56 < |\eta^\gamma| < 1.81$, where it is 7-18%**
- **The uncertainty in the photon identification represents a significant contribution at low E_T^γ: it increases from 1-2% at 125 GeV to 2-6% at $\sim$ 1 TeV**
- **The uncertainty in the correlation between the photon ID variables and the isolation is a significant contribution at low E_T^γ: typically smaller than 2%**

Inclusive isolated-photon cross sections vs NLO QCD

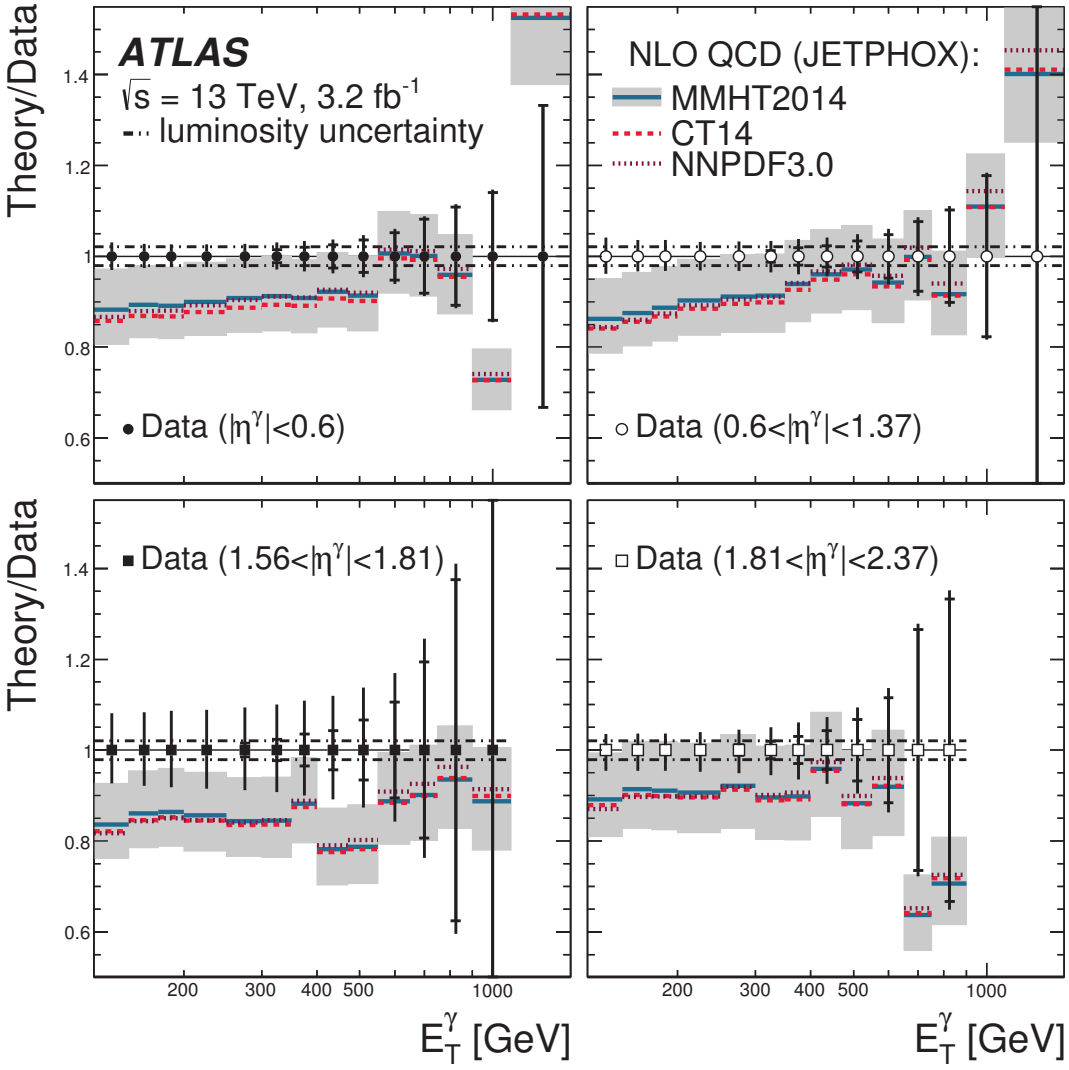

- NLO QCD predictions underestimate data by up to $\approx$ 10-15%
- Theoretical uncertainty 10-15% much larger than experimental uncertainties
- For $E_{\mathrm{T}}^{\gamma} \lesssim 600$ GeV the measurements are systematically limited
- NLO QCD provides an adequate description of the data within uncertainties
- First measurement of inclusive photon production in the new kinematic regime opened by the LHC at $\sqrt{s} = 13$ TeV
- Ready for the comparison to NNLO QCD predictions (Campbell, Ellis, Williams arXiv:1612.04333)

ATLAS Coll., arXiv:1701.06882, accepted PLB

Summary

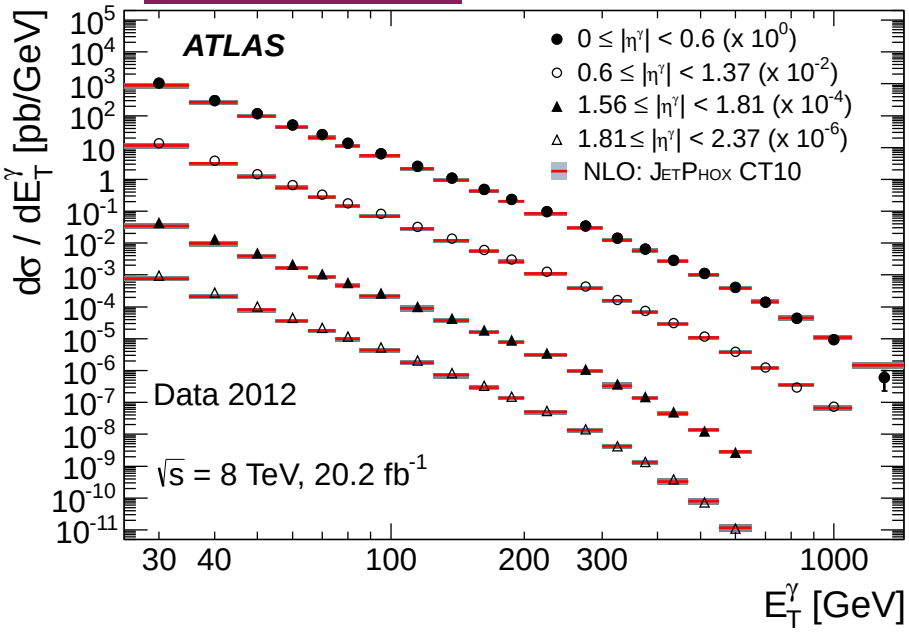

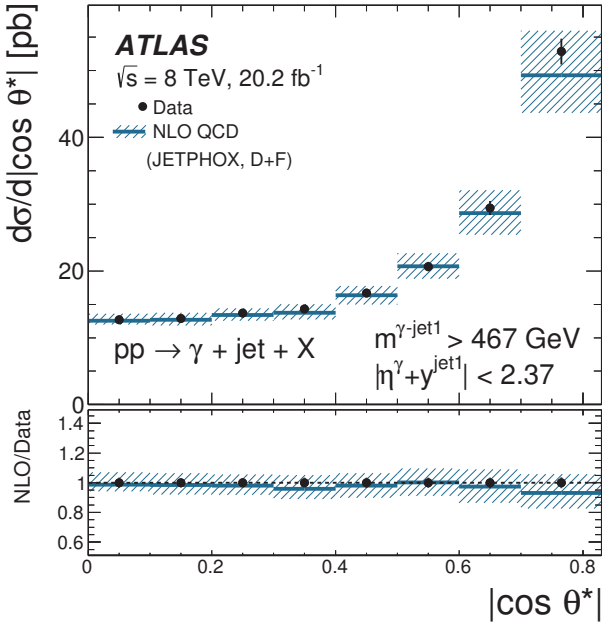

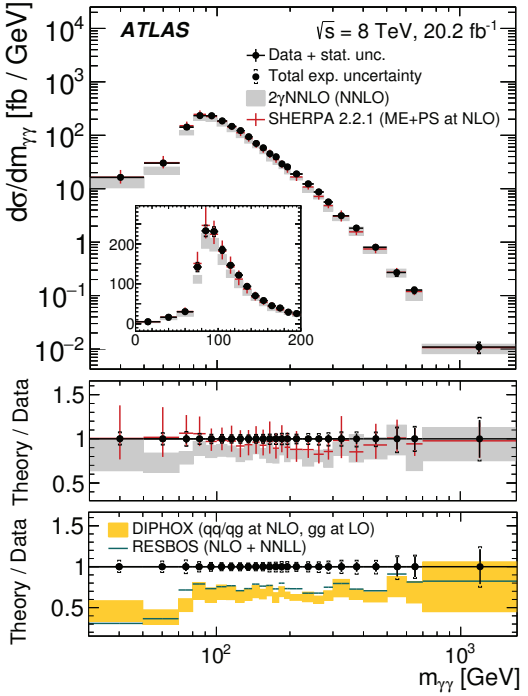

- **Exploration of isolated photon production in pp collisions up to $E_T^\gamma \sim 1$ TeV**
- **Additional experimental information on the gluon density in the proton**
- **Measurement of the dynamics of photon+jet(s) and diphoton production**
- **Understanding (in pQCD) the background to Higgs into $\gamma\gamma$**
- **Overall, perturbative QCD succeeds in describing the data!**

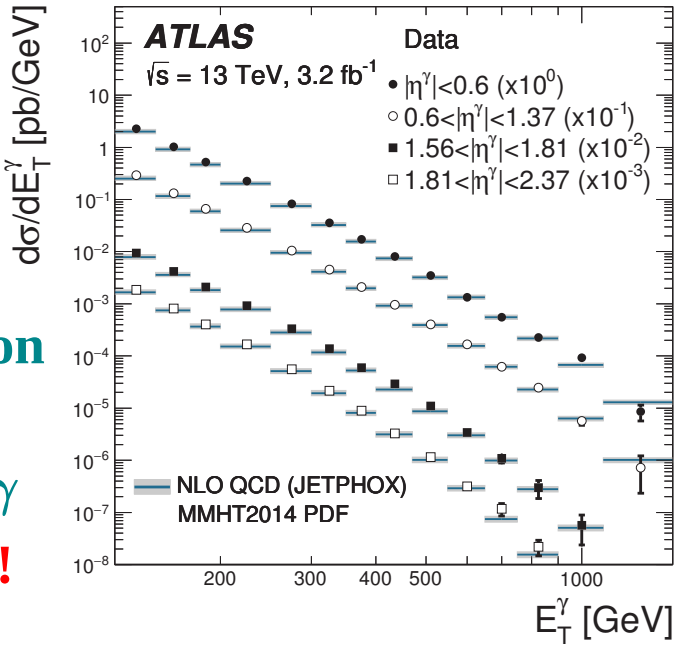

Backup

The ATLAS detector

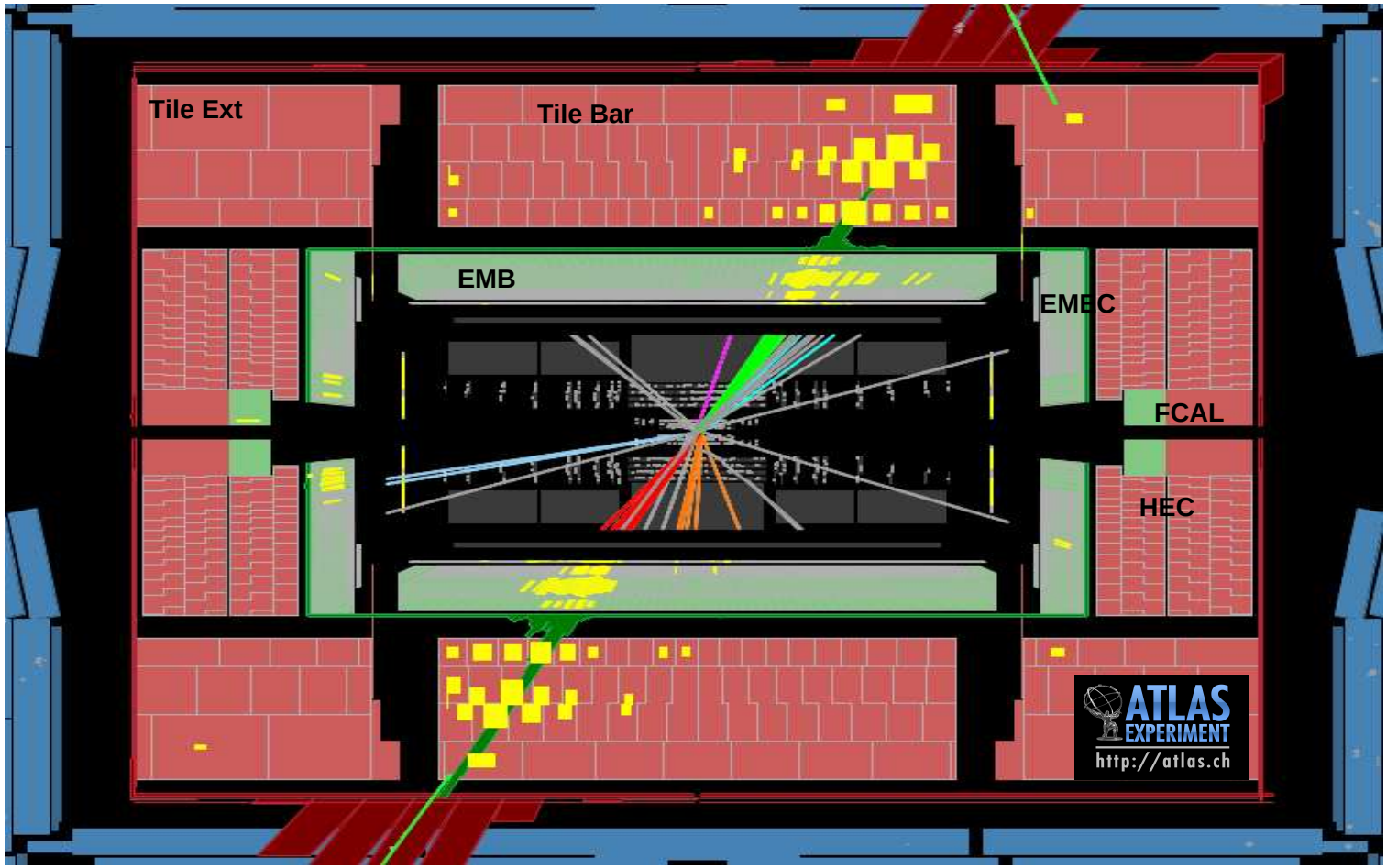

- Inner detector (ID): tracking and particle identification in $|\eta| < 2.5$
- Calorimeters: electromagnetic (LAr) $\rightarrow$ barrel $|\eta| < 1.475$, endcap $1.375 < |\eta| < 3.2$, forward $3.1 < |\eta| < 4.9$; hadronic (scintillator/steel, LAr/Cu, LAr/W) $\rightarrow$ barrel $|\eta| < 0.7$ extended barrel $0.8 < |\eta| < 1.7$, endcap $1.5 < |\eta| < 3.2$ and forward $3.1 < |\eta| < 4.9$

Photon reconstruction in the ATLAS LAr Calorimeter

- Layout of the ATLAS electromagnetic calorimeter (Lead-liquid Argon)

$\rightarrow$ barrel section, $|\eta| < 1.475$
$\rightarrow$ two end-cap sections, $1.375 < |\eta| < 3.2$
$\rightarrow$ three longitudinal layers

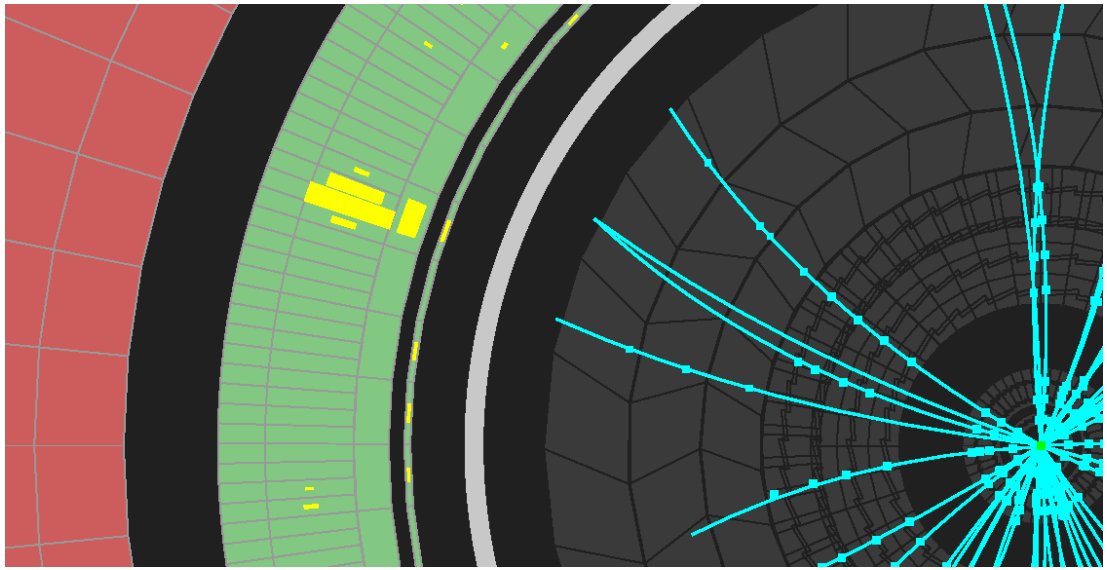

– First layer: high granularity in η direction, width 0.003-0.006 (except for $1.4 < |\eta| < 1.5$ and $|\eta| > 2.4$)

– Second layer: collects most of the energy, granularity 0.025×0.025 in $\eta \times \phi$

– Third layer: used to correct for leakage

- Cluster of EM cells without matching track:
$\rightarrow$ "unconverted" photon candidate

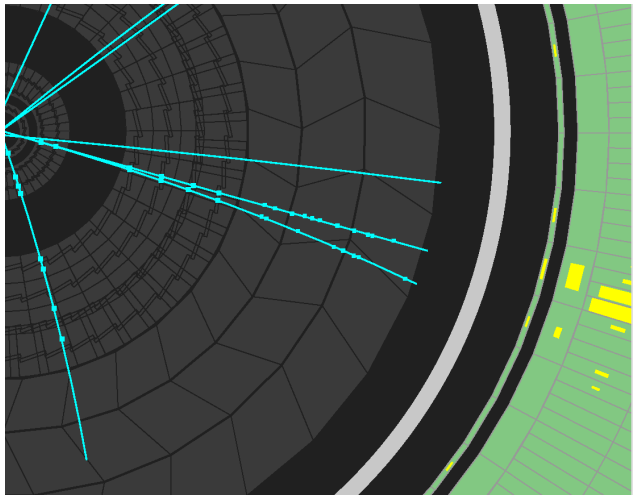

- Cluster of EM cells matched to pairs of tracks (from reconstructed conversion vertices in the inner detector) or matched to a single track consistent with originating from a photon conversion
$\rightarrow$ "converted" photon candidate

Photon identification in the ATLAS LAr Calorimeter

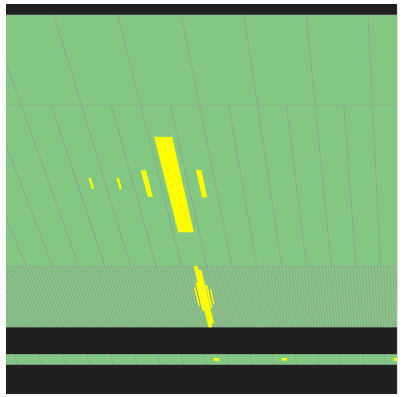

γ

- **To discriminate signal vs background: shape variables from the lateral and longitudinal energy profiles of the shower in the calorimeters; "loose" and "tight" identification criteria.**

- **"Loose" identification criteria:**

$\rightarrow$ leakage $R_{had} = E_T^{had}/E_T$ (1st layer hadronic calorimeter)

$\rightarrow$ $R_\eta = E^{S2}_{3\times7}/E^{S2}_{7\times7}$; $S2$=second layer of EM calorimeter

$\rightarrow$ RMS width of the shower in η direction in $S2$

- **"Tight" identification criteria:**

$\rightarrow$ the requirements applied in "Loose" are tightened

$\rightarrow$ $R_\phi = E^{S2}_{3\times3}/E^{S2}_{3\times7}$

and shower shapes in the first layer (to discriminate single-photon showers from overlapping nearby showers, such as $\pi^0 \rightarrow \gamma\gamma$)

$\rightarrow$ e.g. asymmetry between the 1st and 2nd maxima in the energy profile along η ($S1$)

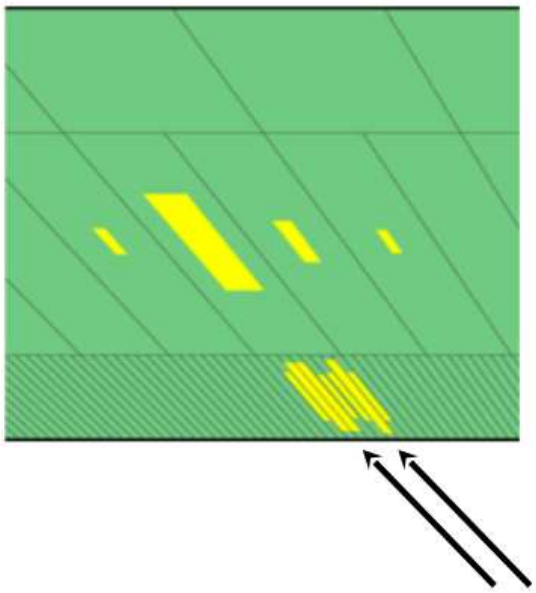

$\pi^0 \rightarrow \gamma\gamma$

Photon identification efficiency

ATLAS Coll., ATLAS-CONF-2012-123

CONVERTED PHOTONS

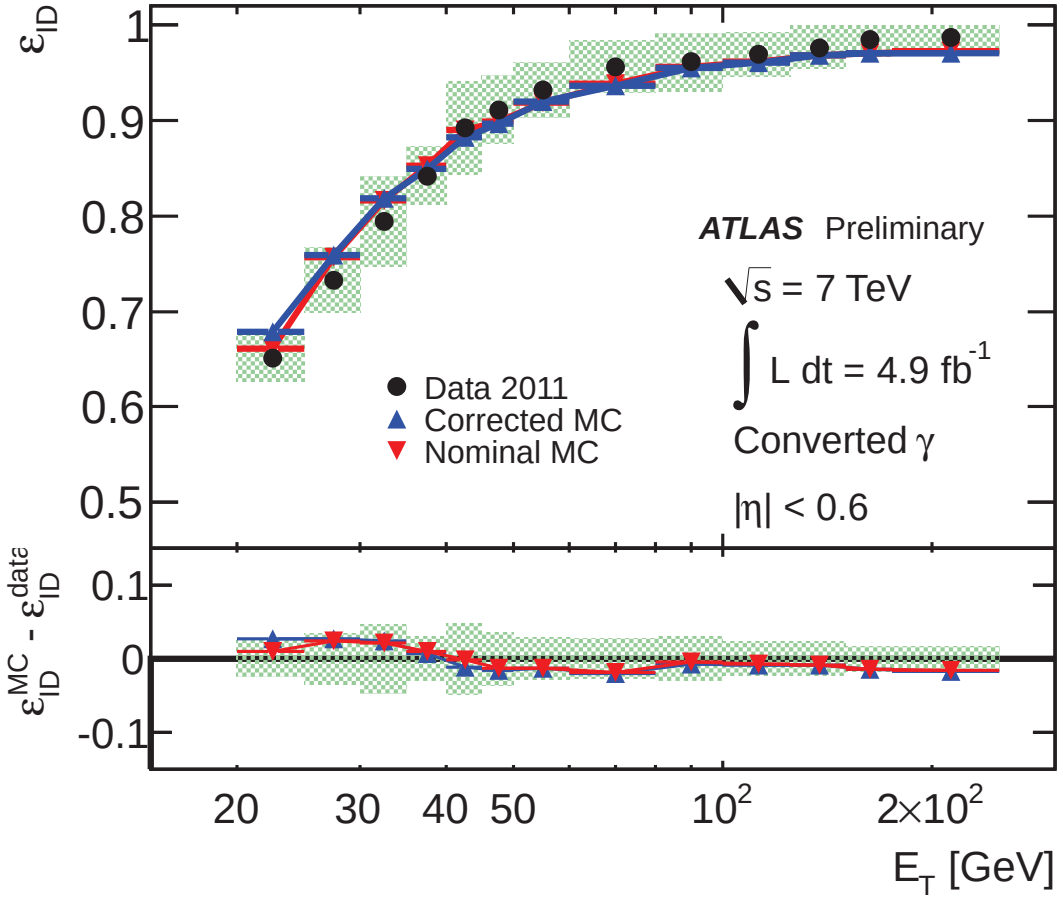

UNCONVERTED PHOTONS

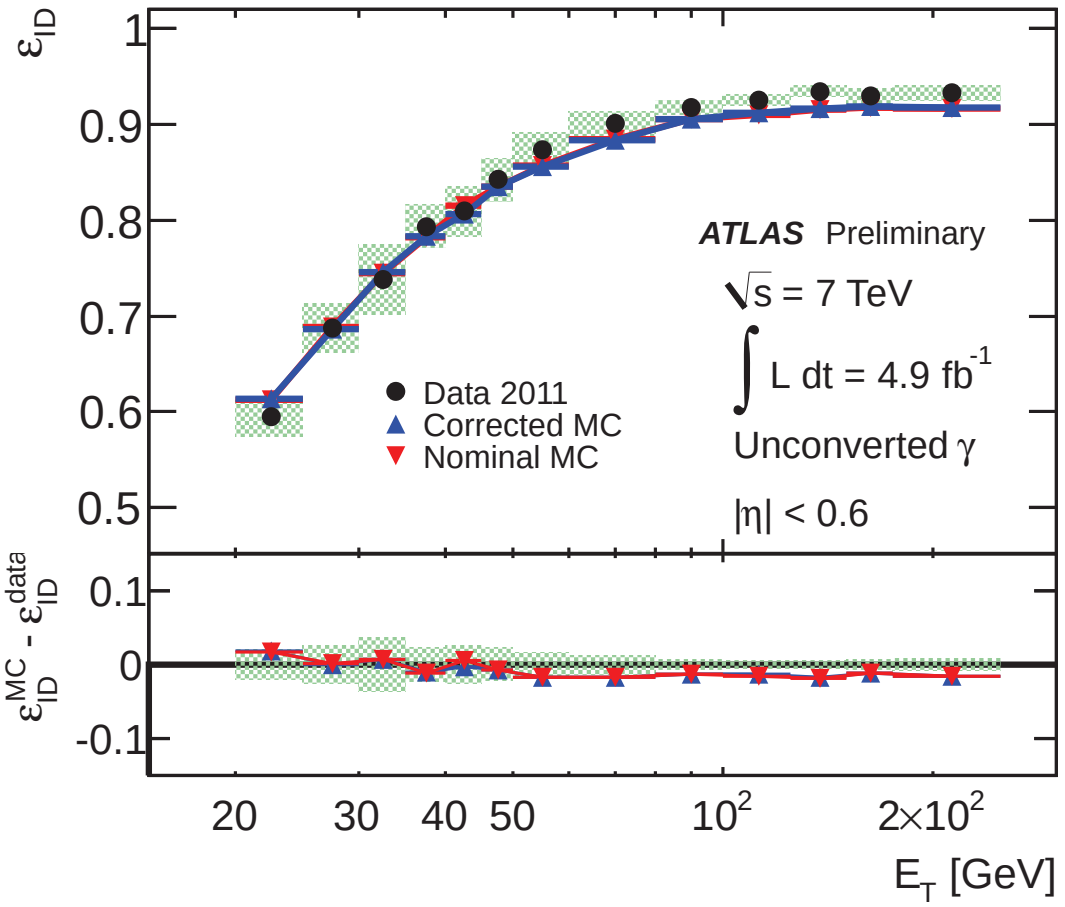

- **Data-driven measurements of photon identification efficiency for converted and unconverted photons (radiative Z decays, extrapolation from $e^{\pm}$ and matrix method) compared to estimations based on Monte Carlo simulations**

Other sources of photons

- Quarks and gluons are sources of photons

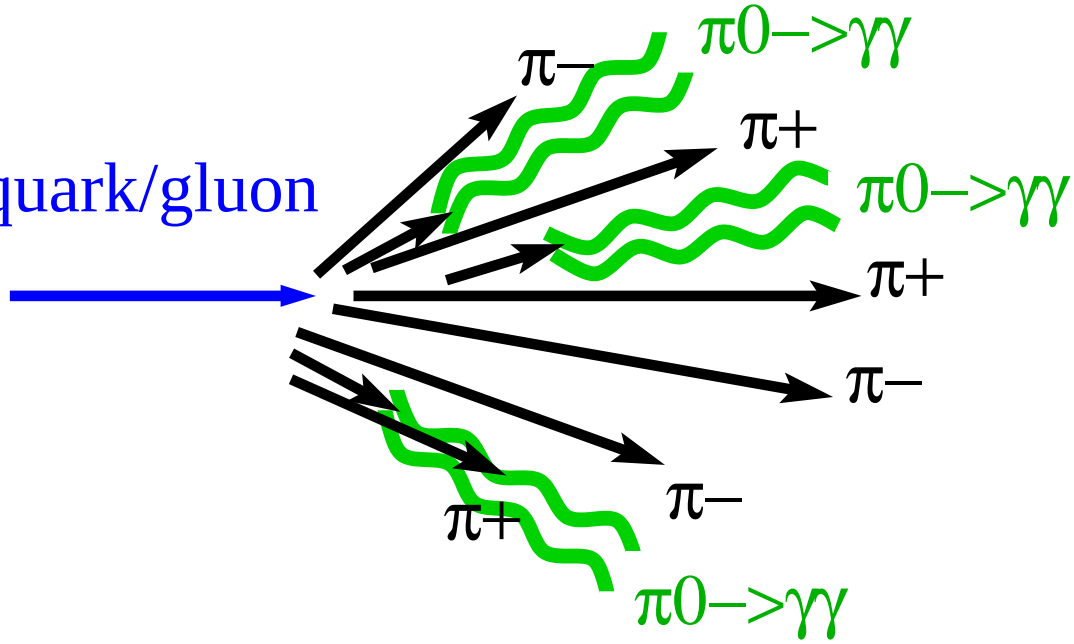

→ Quarks and gluons fragment mostly into pions and, by isospin symmetry, $1/3$ are π^0's, which decay into two photons

⇒ γ's are produced copiously inside jets!

→ Quarks have electric charge and radiate photons

⇒ fragmentation function $D^{\gamma}_{q/g}(z, \mu_f)$

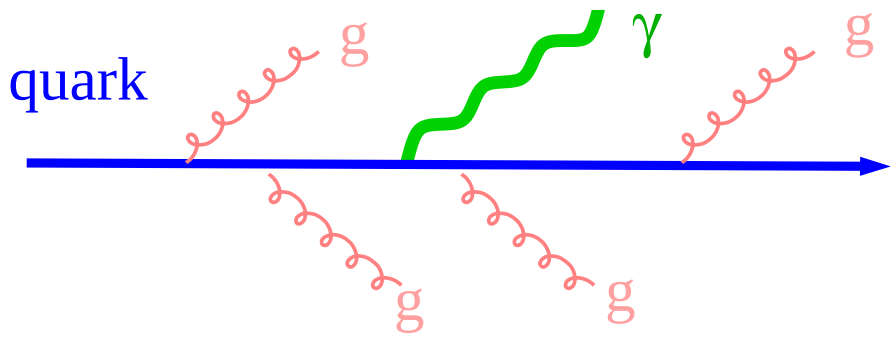

⇒ Distinct feature: these photons are inside jets, i.e. not isolated!

Photon isolation

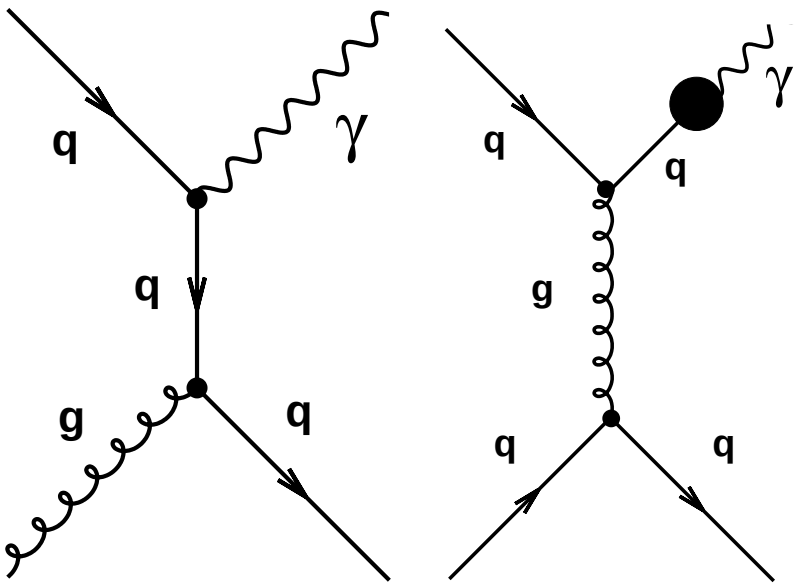

Direct-photon Fragmentation

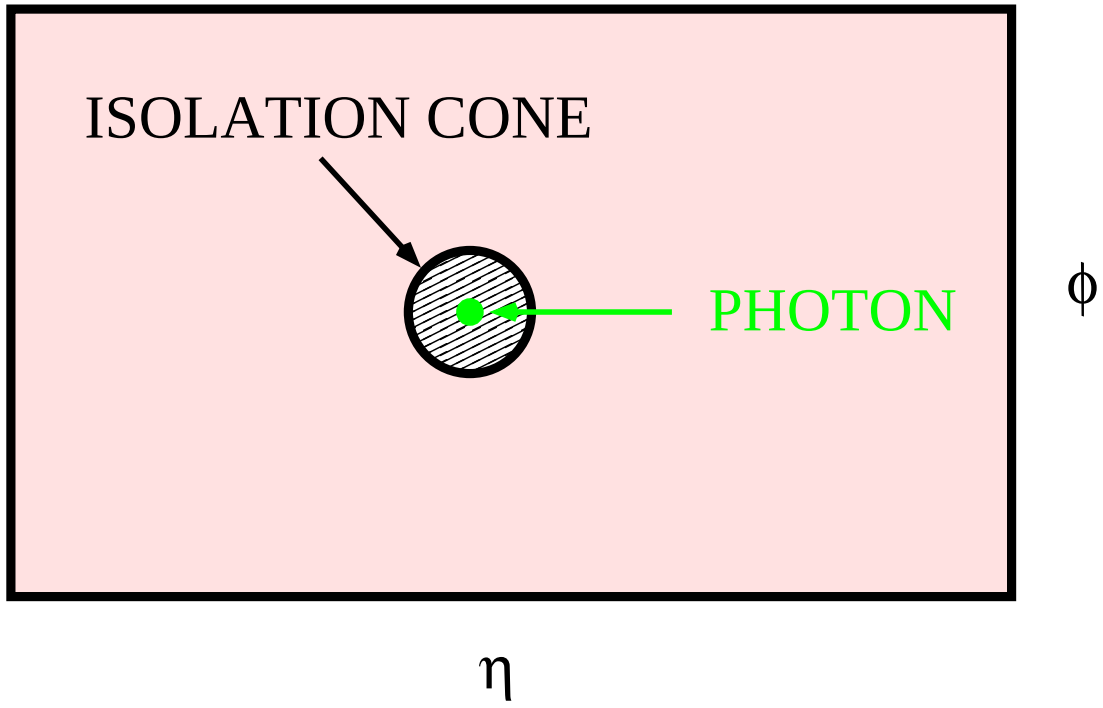

- It is essential to require the photon to be isolated. It is achieved by requiring $E_T^{iso} \equiv \sum_i E_T^i < E_T^{\max}$ with the sum over the particles (except the photon!) inside a cone of radius $R = 0.4$ centered on the photon in the $\eta - \phi$ plane

- The isolation requirement suppresses the contribution of photons inside jets: π^0 (as well as other neutral mesons) decays and the fragmentation contribution

Photon isolation in ATLAS

- $E_T^{iso}(R = 0.4)$ computed using clusters of calorimeter cells (EM and HAD) in a cone $R = 0.4$, excluding the contribution from the photon
- Subtraction of the leakage of the photon energy outside that region (few %)
- The underlying event and pileup (overlapping pp interactions in the same/neighbouring bunch crossings) contribute to E_T^{iso}!
  Subtracted on event-by-event basis using the jet-area method of M. Cacciari et al
- After isolation requirement, residual background still expected

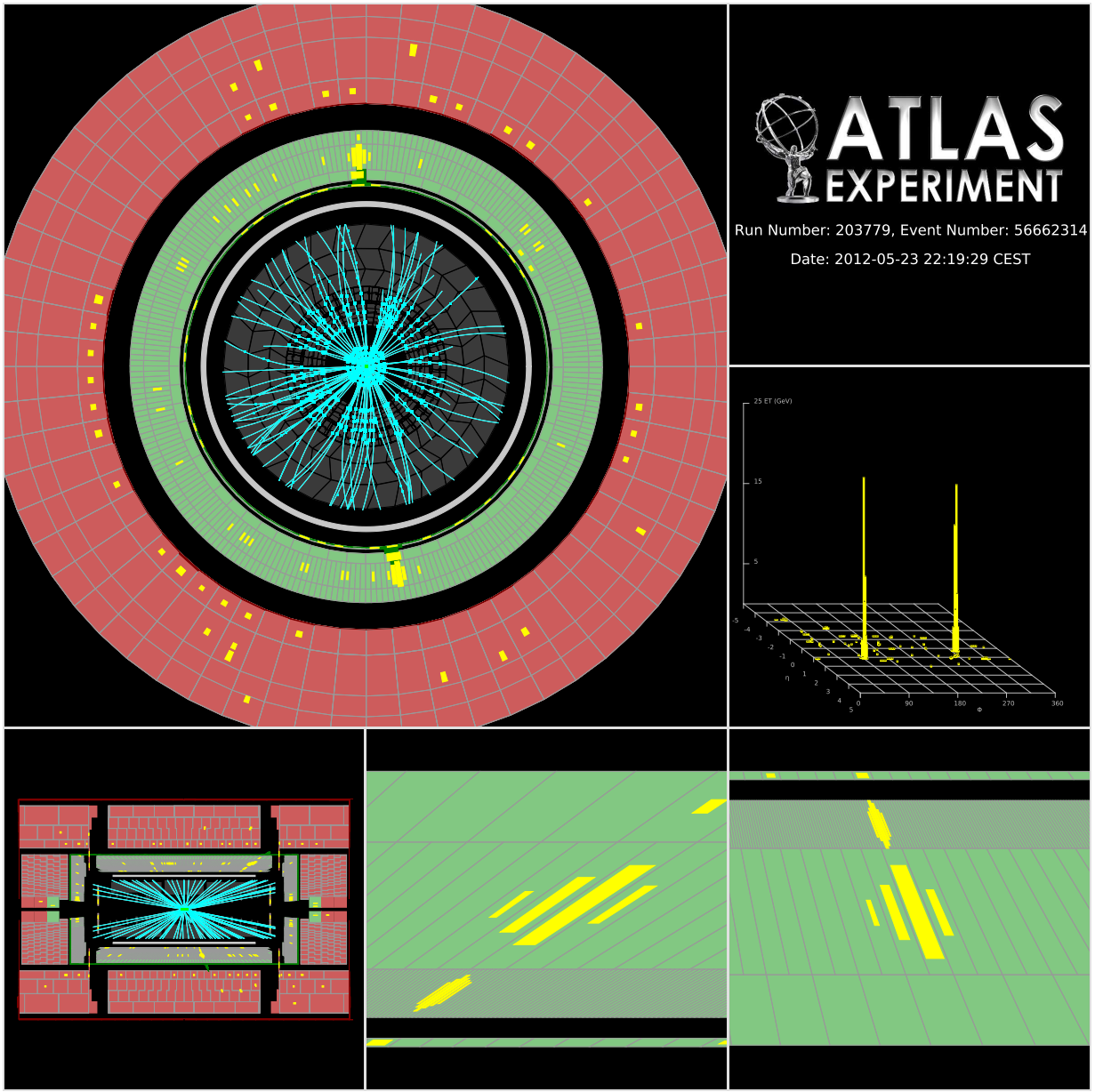

Photon isolation in ATLAS

- E_T^{iso} is corrected by subtracting the estimated contributions from the underlying event and pileup; the correction is computed on an event-by-event basis (to avoid the large fluctuations) using the jet-area method (M. Cacciari et al.)
  $\Rightarrow$ ambient transverse-energy density 540 MeV (in $R = 0.4$ cone) for events with at least one photon candidate with $E_T > 15$ GeV and exactly one PV ($+170$ MeV for each extra PV)
- After the correction the E_T^{iso} distribution is centered at zero with a width of 1.5 GeV in simulated signal events

ATLAS Coll., PRD83 (2011) 052005

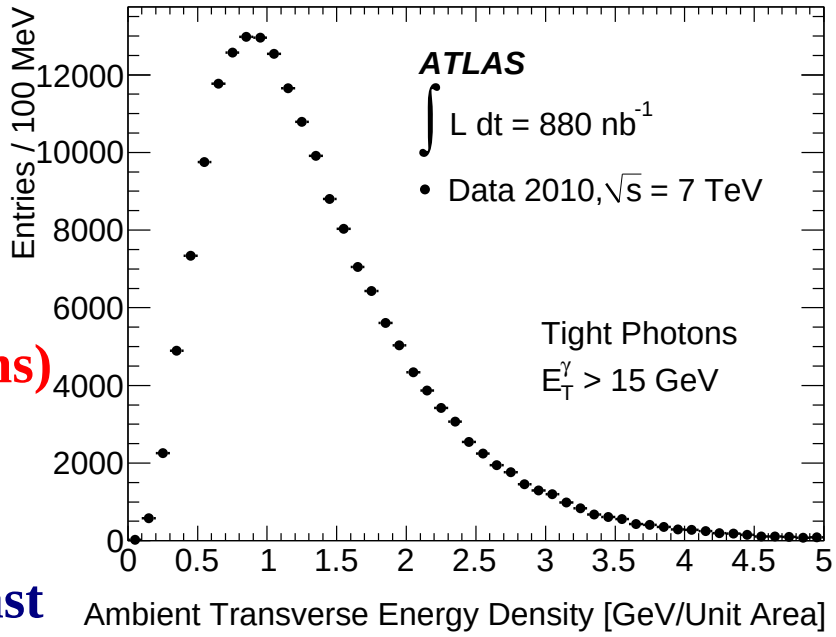

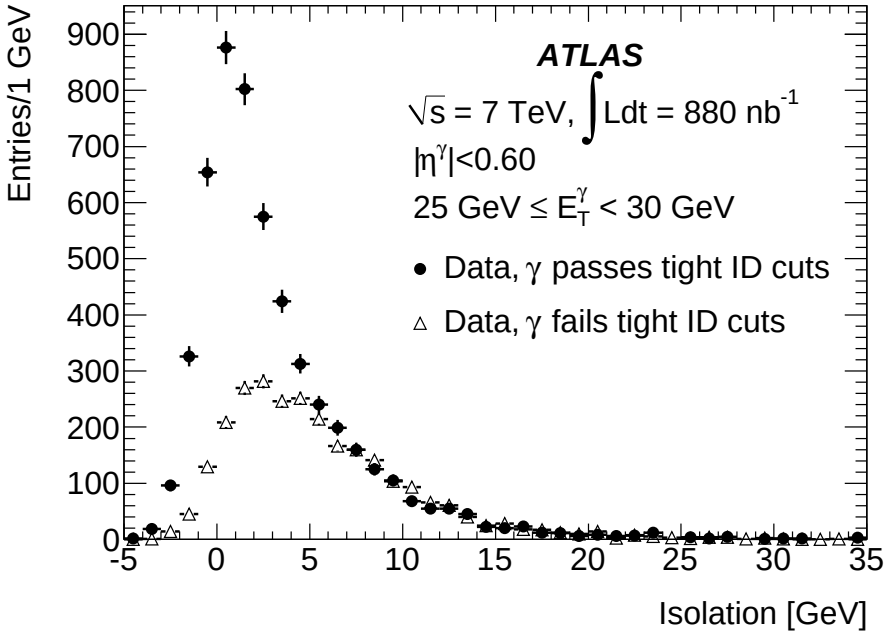

Background subtraction

- **Residual background still expected even after the tight identification and isolation requirements**
- **A data-driven method necessary to avoid relying on detailed simulations of the background processes**
- **The two-dimensional sideband method:**

→ photon identification γ_{ID} vs E_T^{iso} plane

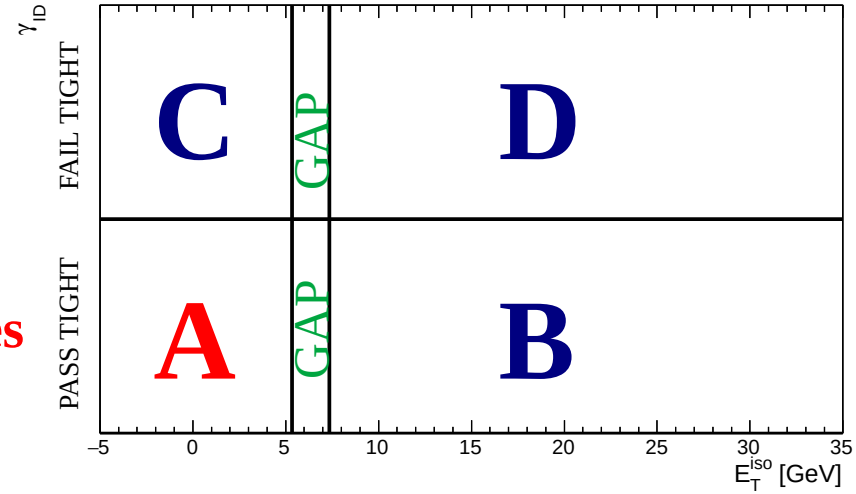

- **It is assumed that for background events there is no correlation between γ_{ID} and E_T^{iso}**

$$\frac{N_A^{bkg}}{N_B^{bkg}} = \frac{N_C^{bkg}}{N_D^{bkg}} \Rightarrow R_{bkg} \equiv \frac{N_A^{bkg} \cdot N_D^{bkg}}{N_B^{bkg} \cdot N_C^{bkg}} = 1$$

and the effects of the small signal contaminations can be accounted for by using

$$\frac{N_A - N_A^{sig}}{N_B - \epsilon_B N_A^{sig}} = \frac{N_C - \epsilon_C N_A^{sig}}{N_D - \epsilon_D N_A^{sig}}$$

to extract the signal yield N_A^{sig}

the leakage fractions ($\epsilon_K \equiv N_K^{sig}/N_A^{sig}, K = B, C, D$) are estimated using MC samples of signal ⇒ purity rises from 60% ($E_T^{\gamma} \sim 25$ GeV) to 100% ($E_T^{\gamma} \sim 300$ GeV)

Diphoton: sample composition and experimental uncertainties

Process	Event fraction [%] Two-dimensional template fit	Matrix method
$\gamma\gamma$	75.3 ± 0.3 (stat) $^{+2.6}_{-2.8}$ (syst)	73.9 ± 0.3 (stat) $^{+3.1}_{-2.7}$ (syst)
γj	14.5 ± 0.2 (stat) $^{+2.7}_{-2.8}$ (syst)	14.4 ± 0.2 (stat) $^{+2.0}_{-2.4}$ (syst)
jγ	6.0 ± 0.2 (stat) $^{+1.4}_{-1.5}$ (syst)	5.8 ± 0.1 (stat) ± 0.6 (syst)
jj	1.6 ± 0.2 (stat) $^{+0.9}_{-0.4}$ (syst)	2.4 ± 0.1 (stat) $^{+0.6}_{-0.5}$ (syst)
ee	2.6 ± 0.2 (stat) $^{+0.9}_{-0.4}$ (syst)	3.5 ± 0.1 (stat) ± 0.4 (syst)

Source of uncertainty	Impact on $\sigma^{\text{fid.}}_{\text{tot}}$ [%]
Photon identification efficiency	± 2.5
Modeling of calorimeter isolation	± 2.0
Luminosity	± 1.9
Control-region definition	$^{+1.5}_{-1.7}$
Track isolation efficiency	± 1.5
Choice of MC event generator	± 1.1
Other sources combined	$^{+0.8}_{-1.3}$
Total	$^{+4.5}_{-4.7}$

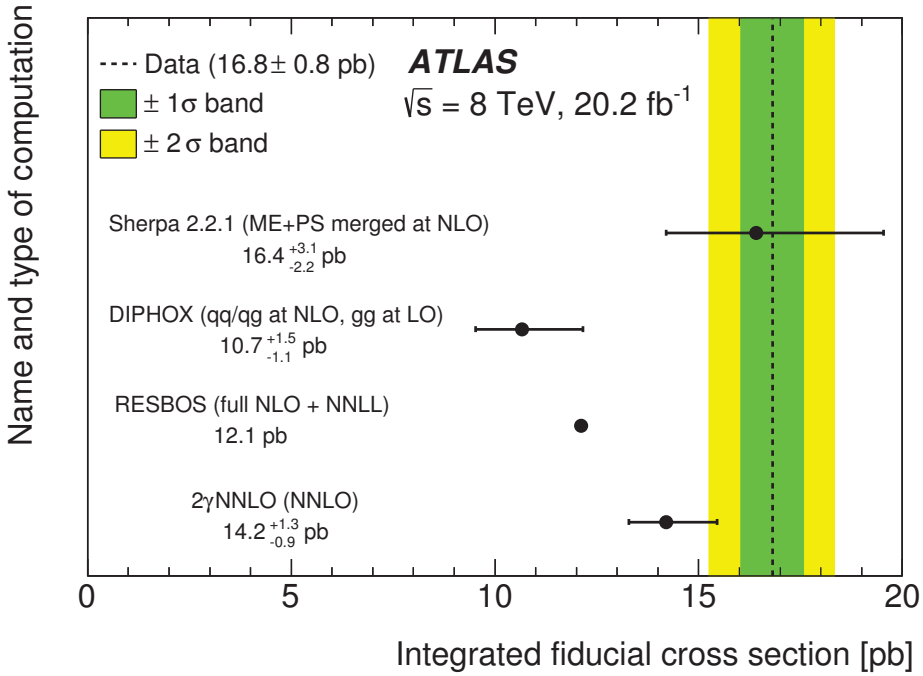

ATLAS Coll., arXiv:1704.03839

Diphoton: E_T^{iso} distributions

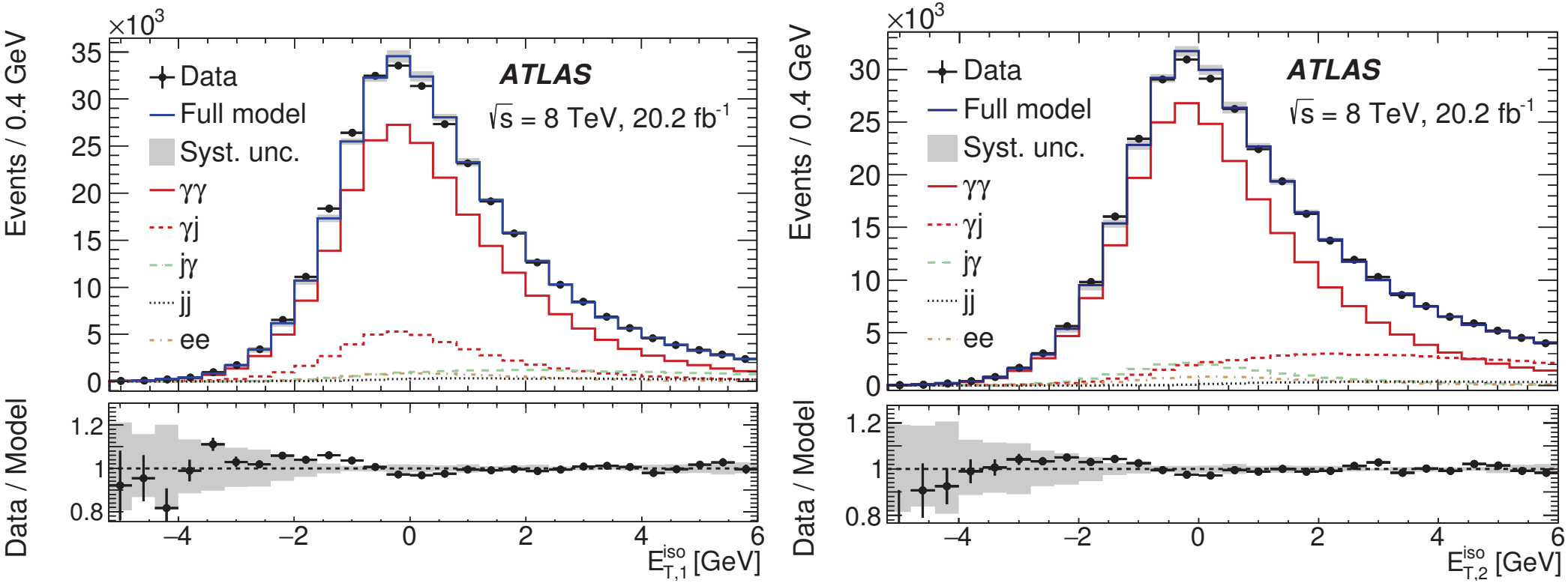

ATLAS Coll., arXiv:1704.03839

Diphoton: sample composition

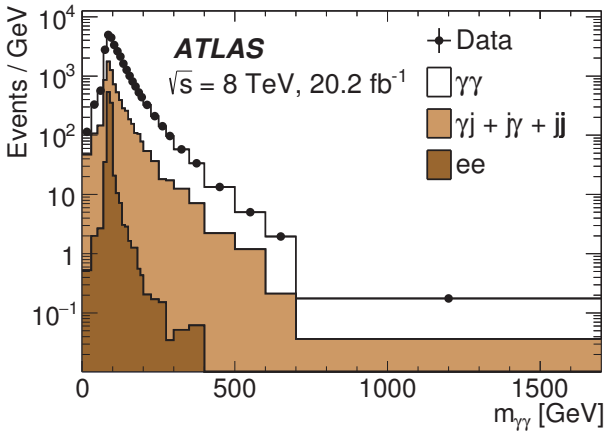

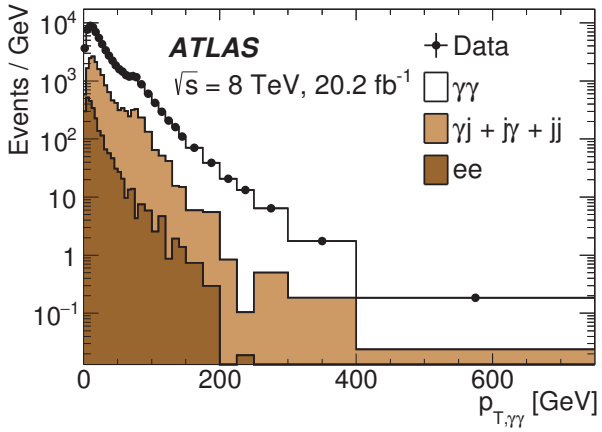

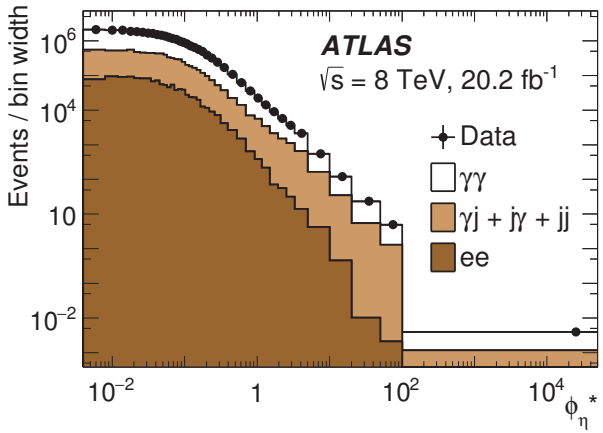

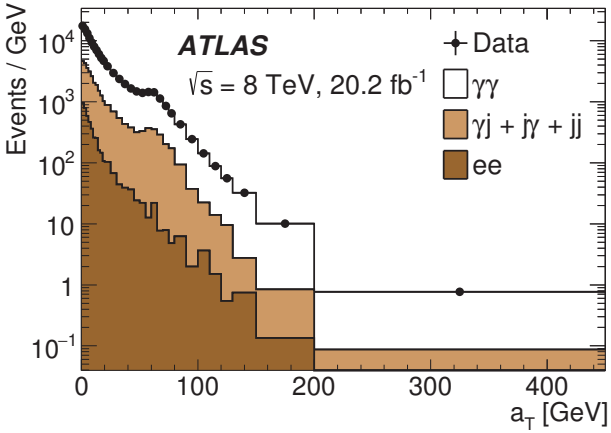

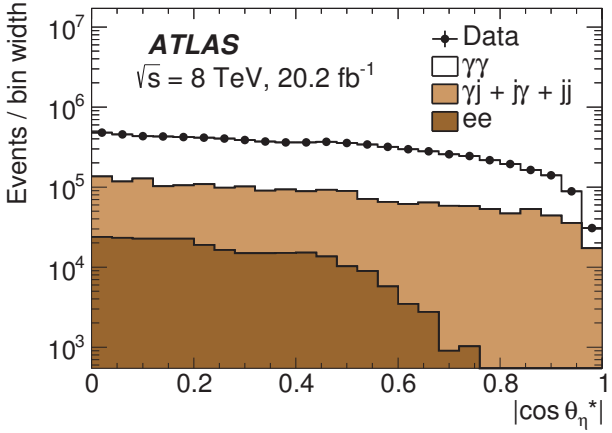

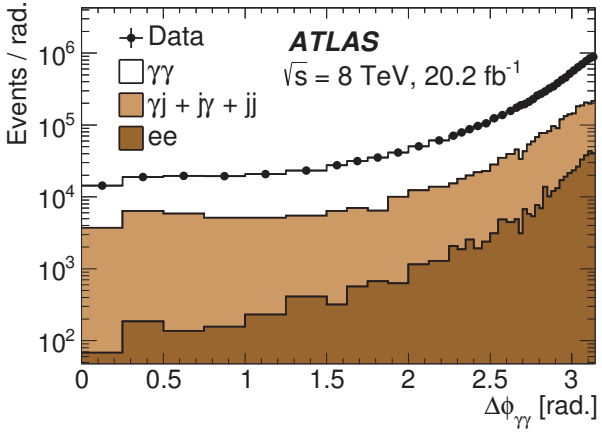

ATLAS Coll., arXiv:1704.03839

Diphoton: experimental uncertainties

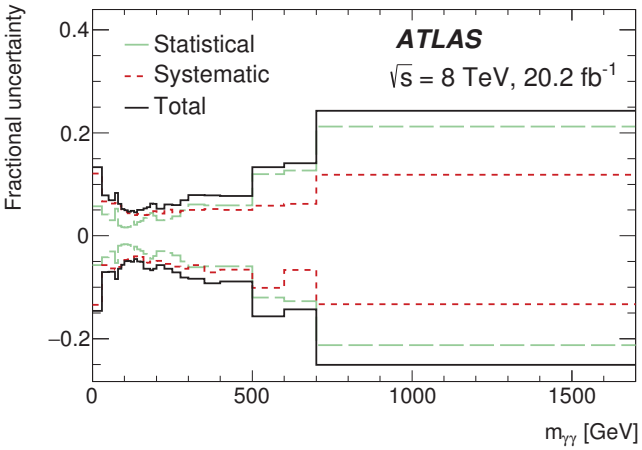

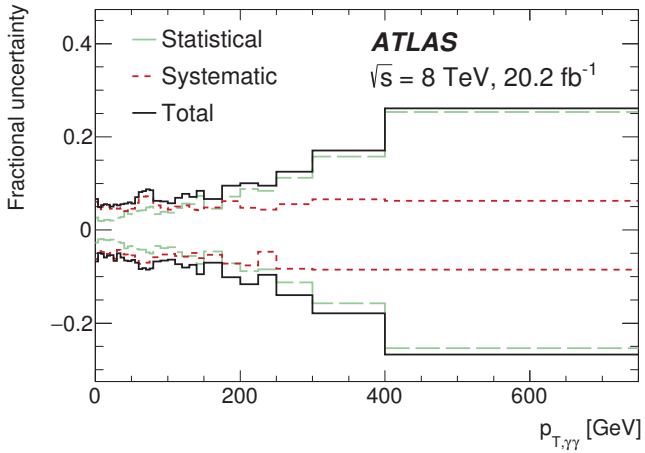

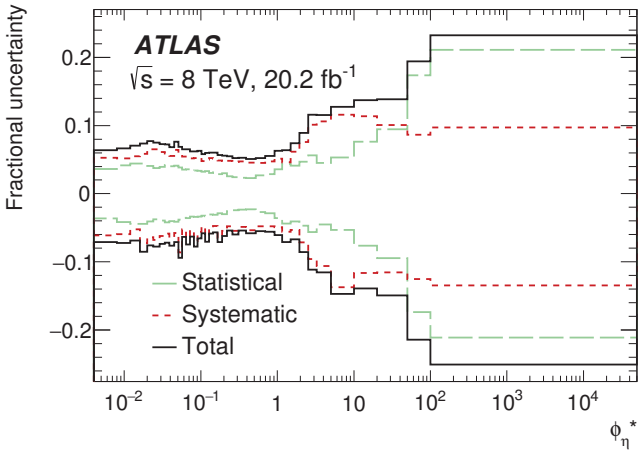

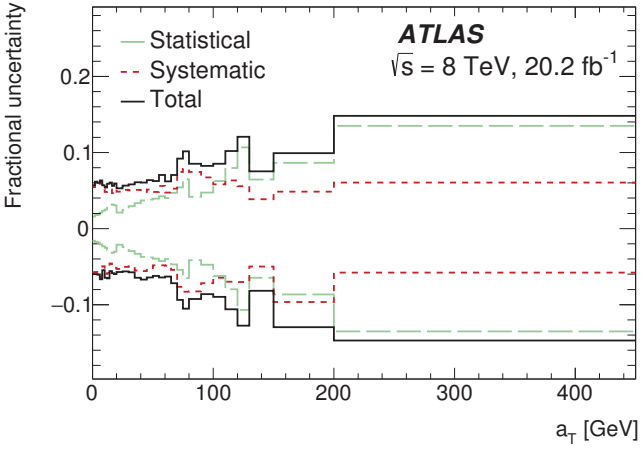

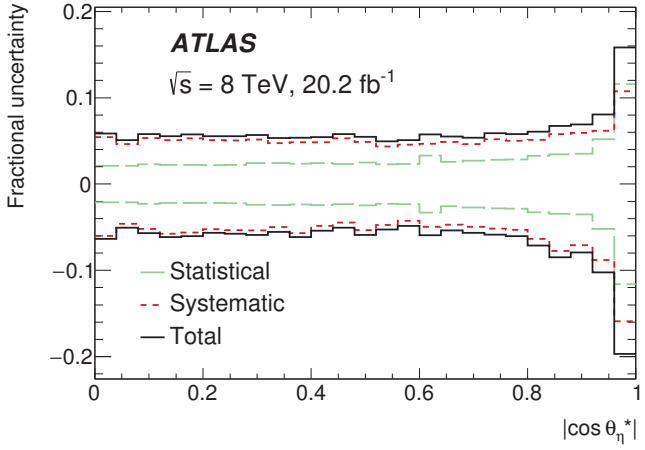

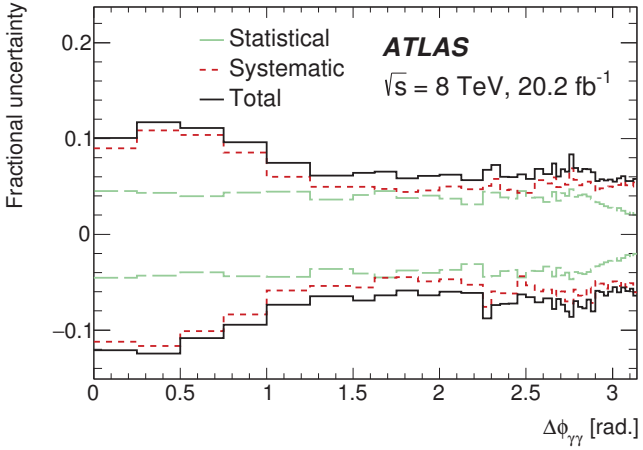

ATLAS Coll., arXiv:1704.03839

NLO QCD calculations for inclusive photon production

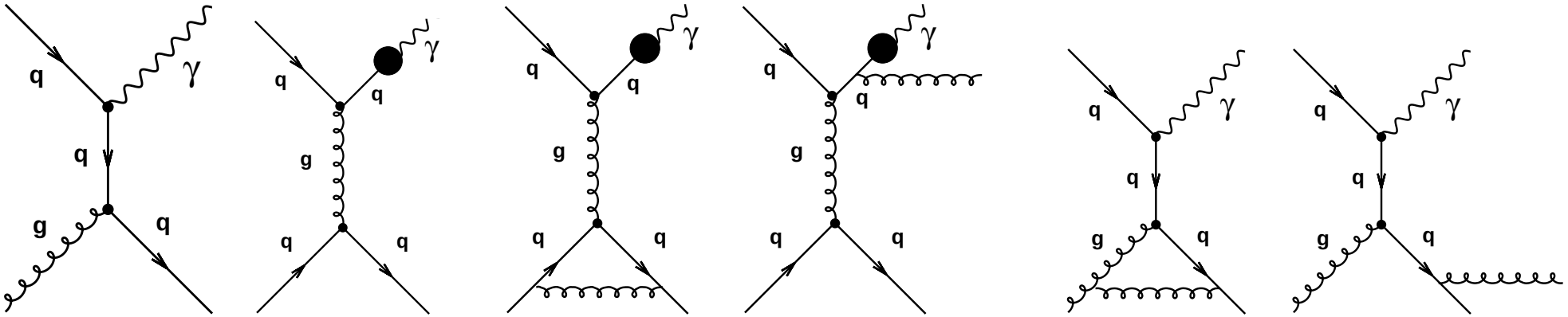

$$\sigma_{pp\to\gamma+X} = \sum_{i,j,a} \int_0^1 dx_1\, f_{i/p}(x_1,\mu_F^2) \int_0^1 dx_2\, f_{j/p}(x_2,\mu_F^2)\; \hat{\sigma}_{ij\to\gamma a} +$$

$$\sum_{i,j,a,b} \int_{z_{min}}^1 dz\, D_a^\gamma(z,\mu_f^2) \int_0^1 dx_1\, f_{i/p}(x_1,\mu_F^2) \int_0^1 dx_2\, f_{j/p}(x_2,\mu_F^2)\; \hat{\sigma}_{ij\to ab}$$

- The calculations includes NLO corrections for both direct-photon and fragmentation contributions; beware the components are not distinguishable beyond LO
- The calculations implement the photon isolation requirement at "parton" level: E_T^{iso} calculated with the (few) final-state partons in the perturbative QCD calculation

NLO QCD calculations for inclusive photon production

$$\sigma_{pp\to\gamma+X} = \sum_{i,j,a} \int_0^1 dx_1\, f_{i/p}(x_1,\mu_F^2) \int_0^1 dx_2\, f_{j/p}(x_2,\mu_F^2)\ \hat{\sigma}_{ij\to\gamma a} +$$

$$\sum_{i,j,a,b} \int_{z_{min}}^1 dz\, D_a^\gamma(z,\mu_f^2) \int_0^1 dx_1\, f_{i/p}(x_1,\mu_F^2) \int_0^1 dx_2\, f_{j/p}(x_2,\mu_F^2)\ \hat{\sigma}_{ij\to ab}$$

- **Using the JetPhox program (S. Catani, M. Fontannaz, J. Ph. Guillet and E. Pilon) with**
  - $\to$ $\mu_R = \mu_F = \mu_f = E_T^\gamma$ **(nominal)**
  - $\to$ **proton PDF set: CT10**
  - $\to$ **fragmentation function: BFG set II**

$\to$ **Corrections for hadronisation and underlying event needed**

- **Theoretical uncertainties:**

$\to$ **terms beyond NLO; varying μ_R, μ_F, μ_f by factors 2 and $1/2$ (singly or simultaneously)**

$\to$ **PDF-induced uncertainties; estimated using set of PDF eigenvectors**

$\to$ **uncertainty on α_s; estimated using PDFs in which different values of α_s are assumed**

$\to$ **uncertainty on non-perturbative correction; estimated with different MCs**

Corrections for non-perturbative effects; photon isolation

- The measurements are corrected for detector effects to the "particle" level
  → to isolated photons, where E_T^{iso} is calculated using all the final-state particles and the jet-area method is also applied
  This is performed using MC simulations

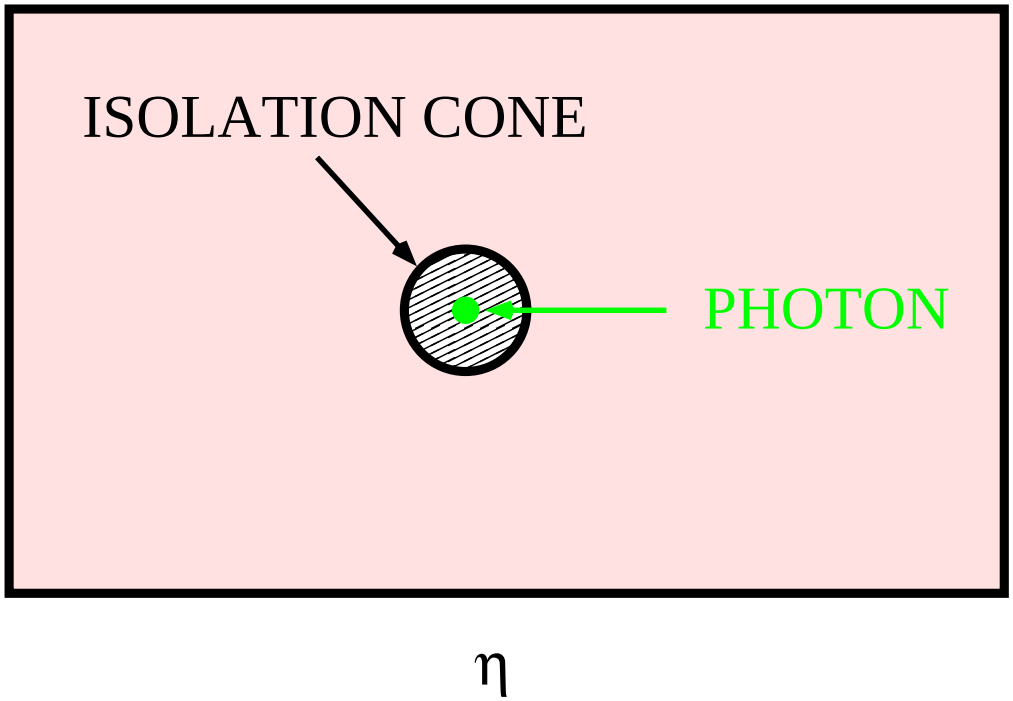

- Corrections for non-perturbative effects (hadronisation and underlying event)

$$C_{NP} = \frac{\sigma_{\gamma+\mathrm{X}}(\mathrm{MC, particle-level, UE})}{\sigma_{\gamma+\mathrm{X}}(\mathrm{MC, parton-level, no\ UE})}$$

→ Less dependence on the modelling of the final state by having used the jet-area method to subtract the "extra" transverse energy contribution to E_T^{iso}

Impact of inclusive isolated photon measurements at LHC on PDFs

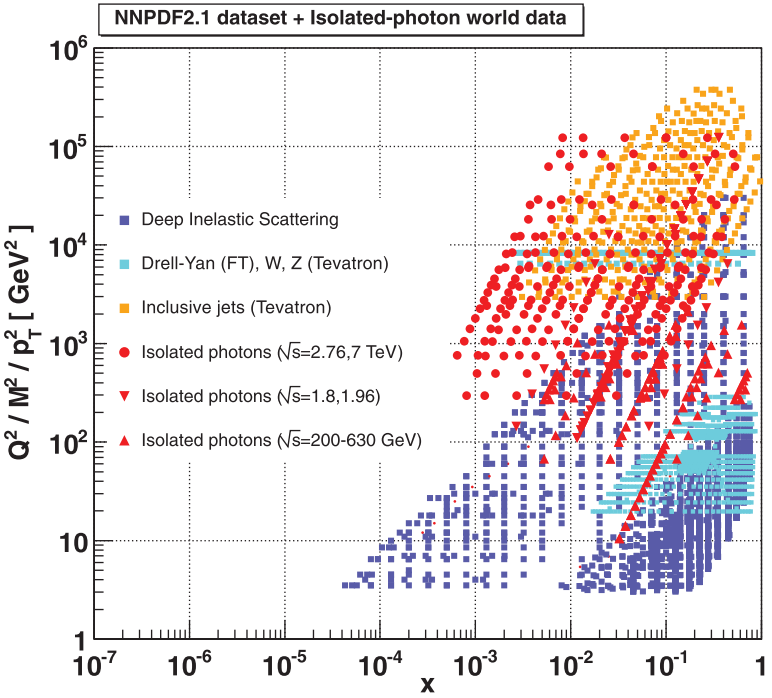

- **Analysis by D. d'Enterria and J. Rojo (NPB860,2012,311)**
- **Study of the impact on the gluon density of existing isolated-photon measurements from a variety of experiments, from $\sqrt{s} = 200$ GeV up to 7 TeV**
  - **$\rightarrow$ those at LHC are the more constraining datasets**
  - **$\rightarrow$ reduction of gluon uncertainty up to 20%**
  - **$\rightarrow$ localised in the range $x \approx 0.002$ to 0.05**

$\Rightarrow$ improved predictions for low mass Higgs production in gluon fusion, PDF-induced uncertainty decreased by 20%